THE PETROLEUM SYSTEM IN THE SANDINO FOREARC BASIN, OFFSHORE WESTERN NICARAGUA

I. Struss[a*], V. Artiles[b], B. Cramer[c] and J. Winsemann[a]

The underexplored Sandino Basin (Nicaragua Basin/Trough) is located within the forearc area of western Nicaragua and NW Costa Rica. Exploration activity since 2004 has focussed on the onshore sector of the basin, and has included the first drilling campaign for over 30 years. Recent 2D basin modelling of the offshore sector together with organic geochemical studies has attempted to reassess the basin's petroleum potential. Geochemical data from the deepest offshore well indicate that Middle Eocene to Lower Oligocene sediments of the Brito Formation, as well as Upper Oligocene to Lower Miocene sediments of the Masachapa Formation, may have source rock potential. A third and perhaps more significant potential source rock interval is associated with the Lower Cretaceous black shales of the Loma Chumico Formation, which has been studied in the adjacent forearc area in NW Costa Rica (Tempisque Basin) and is inferred to be present in the Sandino Basin.

The thermal history of the forearc basin is controlled by the low basal heat flow (39 mW/m^2). 2D modelling has shown that the Sandino Basin is thermally mature, resulting in the potential for hydrocarbon generation in organic-rich intervals in the Brito and Masachapa Formations. A petroleum-generating "kitchen" has tentatively been identified on a NE-SW seismic section which crosses the basin. Modelling suggests that this kitchen has been active from the Late Eocene until the present day, and that the main phases of petroleum generation in general coincide with phases of maximum subsidence in the Late Eocene, Late Oligocene and Plio-Pleistocene. Hydrocarbon migration most probably occurred from the deep basin towards the flanks. Significant volumes of petroleum may have been lost prior to the Late Miocene before the formation of a coastal flexure which can be recognised in the NE of the seismic profile.

INTRODUCTION

Petroleum exploration in the Sandino forearc basin (Fig. 1 B) (formerly referred to as the Nicaragua Trough or Nicaragua Basin: Weyl, 1980; Astorga, 1988; Winsemann and Seyfried, 1991; Winsemann, 1992) began in the early part of the 20th century, but the petroleum system is still poorly understood. The first well was drilled in Nicaragua in 1930 but political and environmental factors have until recently hampered exploration efforts, and at present the country imports all of its energy requirements. However, the presence of live oil seeps at the Citalapa River near the town of San Cayetano (40 km SW of Managua: Fig. 1B), together with oil and gas shows in a number of exploration wells, point to the presence of an active hydrocarbon system. A recent change of government policy has resulted in renewed exploration interest in Nicaragua.

Exploration in the Sandino Basin has been relatively limited due mainly to the basin's forearc setting and the consequent low geothermal gradient. Previous studies have focussed on the basin's tectonic evolution and the nature of the basement (e.g. Crowe and Buffler, 1985; von Huene and Flueh, 1994; Protti *et al*., 1995; Ranero *et al*., 2000 a;b; Walther *et al*.,

[a] Institute of Geology, Leibniz University Hannover, Callinstrasse 30, 30167 Hannover, Germany.
[b] Ministerio de Energía y Minas, Dirección Petrolero, PO Box: CJ-159, Managua, Nicaragua.
[c] Federal Institute for Geosciences and Natural Resources Hannover (BGR), Stilleweg 2, 30655 Hannover, Germany.

*Corresponding author. email: imks@statoilhydro.com
Present address: StatoilHydro ASA, Research Center, PO Box 7200, 5020 Bergen, Norway.

Key words: Numerical basin modelling, Sandino Basin, Nicaragua, forearc basin, petroleum generation, reaction kinetics.

2000; McIntosh *et al*., 2002). The main exploration efforts in the basin began in 1965 initially in an offshore area operated by Esso and Oceanic Exploration Co. 2D seismic data were acquired over the offshore shelf and four exploration wells were drilled, of which two had oil and gas shows. Onshore, two wells were drilled by Superior Oil Co., both of which had gas shows. In 1990, Western Geophysical acquired new 2D seismic data and reprocessed older data as part of a promotional campaign carried out jointly with Statoil and Geco-Prakla. In the following years, the Norwegian Agency for Development Cooperation (NORAD) supported onshore sedimentological studies which were carried out by the Insituto Nicaragüense de Energía (INE) and the Refinadora Costarricense de Petroleo (RECOPE), and which included organic geochemical as well as biostratigraphic analyses. In 2005/2006, the Norwood/Oklanicsa partnership acquired 430 km of 2D seismic data from the onshore part of the Sandino Basin. More recently, gas, condensate and light oil were encountered during the first onshore drilling operations.

The aims of this study are to reassess the petroleum system in the Sandino Basin, and to investigate the timing of hydrocarbon generation and migration from potential source rocks. For this purpose, organic geochemical analyses and a numerical basin modelling study were carried out. 2D basin modelling using PetroMod (*IES Aachen*) made use of a previously-published reflection seismic line (Ranero *et al*., 2000 b). The seismic section is located in the offshore sector of the Sandino Basin (Fig. 1 B) and was acquired by Western Geophysical in 1990. It was reinterpreted by Ranero *et al.* (2000 b) who used it to study the structural evolution of the Sandino Basin. The line crosses a deep basin in the NE which has been a depocentre since the early stages of forearc evolution (Fig. 2). In the middle part of the section, an area of tectonic deformation is present including the Argonaut and Corvina anticlinal structures. To the SW, the line crosses a near-horizontal shelfal area with decreasing sediment thicknesses and faulting. Its termination in the SW crosses an outer high over a distance of c.10 km. In this area the basement is at a shallow level and the seafloor is slightly flexured (Ranero *et al*., 2000 b). The line crosses the offshore wells *Corvina-2* (total depth [T.D.] 3,666 m) and *Argonaut-1* (T.D. 1,554 m) which were drilled on the Corvina and Argonaut anticlines, respectively (Fig. 2B). Close by are the *Triton-1* (T.D. 2,748 m) and *Corvina-1* (T.D. 1,376 m) boreholes (Figs. 1B, 3).

To evaluate the quantity, quality and maturity of organic matter along this seismic line, a total of 63 cuttings samples from the deepest offshore well were made available. From these materials, reaction kinetic parameters for petroleum generation, such as the activation energy distribution, frequency factors and generation potential, were processed using BGR's proprietary software *Pyrocalc*. The reaction kinetics were utilised to improve the accuracy of hydrocarbon generation modelling within the Sandino Basin. The results improve our understanding of the petroleum system in the Sandino Basin, but quantitative aspects relating to petroleum migration and reservoir saturation are lacking. This is mainly due to the limited availibility and quality of data. In future, renewed exploration activity may permit a basin-wide assessment of the petroleum potential.

GEOLOGICAL SETTING AND STRATIGRAPHY

The Sandino Basin is located in the forearc area of the Central American arc-trench system which extends along southern Mexico and the Central American isthmus. The forearc is controlled by the subduction of the Cocos and Nazca Plates beneath the Caribbean Plate at the Middle America Trench (Fig. 1). Basin evolution started in Late Cretaceous times and continues at the present day (Seyfried *et al*., 1991; Darce *et al*., 2000a; Ranero *et al*., 2000b; Walther *et al*., 2000). Walther *et al.* (2000) proposed that collision of an oceanic plateau with the continental margin in the Late Cretaceous led to the cessation of subduction and to the development of a new subduction zone in Eocene to Oligocene times. The Sandino Basin subsequently developed above the inactive trench between the oceanic plateau to the SW and the continental margin to the NE. Accordingly, activity of the former volcanic arc ceased and it migrated by some 70 km to the SW to its present-day position (Astorga, 1997). The basement of the Sandino Basin is therefore thought to consist of oceanic crust and upper mantle, interpreted to represent a relict of the former subduction zone.

The Sandino Basin covers the present-day coastal plain, continental shelf and slope of western Nicaragua and NW Costa Rica (Fig. 1B). It covers an area of approximately 29,000 km^2 of which 5,000 km^2 are onshore. The basin has a length (NW-SE) of about 250 km and is approximately 100 km wide. The poorly-known northern basin margin is assumed to be located in the Gulf of Fonseca. To the south, the basin is bounded by the Hess Escarpment (Winsemann, 1992; Ranero *et al*., 2000b; Walther *et al*., 2000); in the west, it is bounded by an outer arc high (Darce *et al*., 2000a; Ranero *et al*., 2000b), and to the NE and east, by the Nicaragua Graben (Weyl, 1980; Astorga *et al*., 1991) which developed in the Miocene. Before the Miocene, the Sandino Basin extended further eastwards.

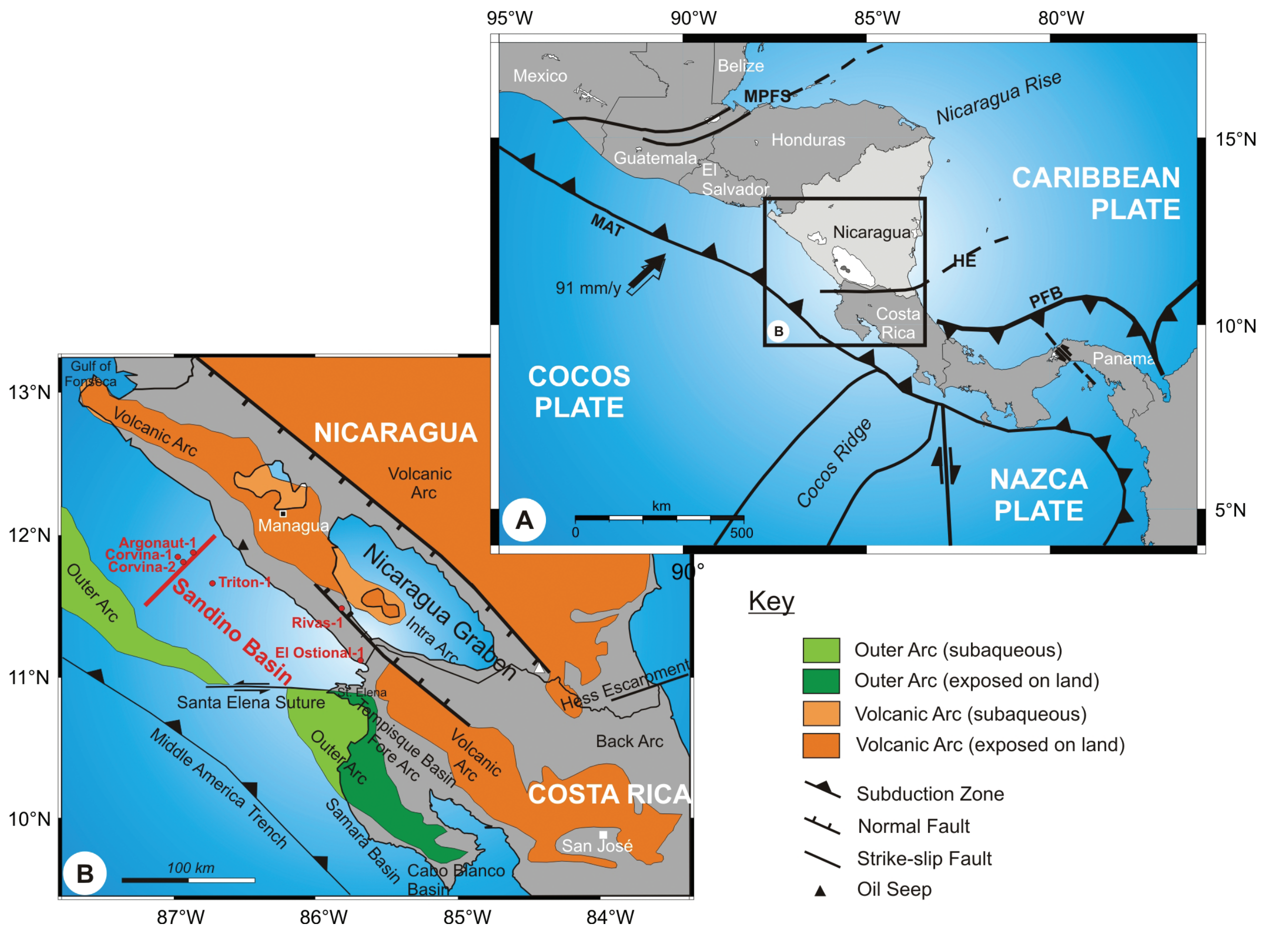

Fig. 1A. Location and plate tectonic setting of the study area. MAT: Middle America Trench; PFB: Panama Foldbelt; MPFS: Motagua-Polochic Fault System; HE: Santa Elena - Hess Escarpment (modified from Pindell and Barett, 1990; Walther *et al.*, 2000). (B) Geological setting of the Sandino Basin (modified from Astorga, 1988; Krawinkel *et al.*, 2000; and Struss *et al.*, 2007). Red solid line illustrates location of the seismic profile investigated; red dots represent borehole locations; black triangle indicates the location of the oil seep at the Citalapa River; white triangle indicates Nicoya Complex rocks cropping out at the San Juan River near Los Sábalos.

In general, the basin succession is about 10 km thick but in the central and northern parts of the basin, sedimentary thicknesses locally exceed 13 km (e.g. Ranero *et al*., 2000b; Walther *et al*., 2000). The oldest sedimentary rocks in the Sandino Basin are of Late Cretaceous age and the fill is dominated by volcaniclastics derived from the volcanic arc to the NE (Kumpulainen *et al*., 1999). The succession is partly exposed along the Pacific coastline of Nicaragua and Costa Rica as a result of regional deformation possibly caused by a major plate reorganization or as a response to changes in subduction rate and angle (Handschumacher, 1976; Weinberg, 1992; Mann and Kolarski, 1995). As a consequence, the basin's depocentre began to migrate to the west. Uplift started in the Late Miocene and continued along parts of the central coast until the Late Pleistocene (Ranero *et al*., 2000b).

The Cretaceous to Tertiary succession can in general be divided into five major formations of mostly deep-water origin (e.g. Weyl, 1980; Astorga, 1988; 1990; Kolb, 1990; Kolb and Schmidt, 1991; Winsemann and Seyfried, 1991; Winsemann, 1992; Krawinkel and Kolb, 1994; Kumpulainen, 1995; Kumpulainen *et al*., 1999). A Late Cretaceous to Early Miocene deep-water succession comprising the Rivas, Brito and Masachapa Formations is unconformably overlain by the Middle Miocene to Pleistocene shallow-water and coastal El Fraile and El Salto Formations. The succession starts with deep-marine volcaniclastic rocks of the Maastrichtian to Palaeocene Rivas Formation (cf. Joy, 1941, cited in Hoffstetter *et al*., 1960; Galli-Olivier and Schmidt-Effing, 1977), which is dominated by turbiditic tuffaceous shales and sandstones with limestone intervals and marls (Weyl, 1980). This formation is poorly exposed at the surface but similar sedimentary rocks are reported in the subsurface at wells *Rivas-1* and *El Ostional-1* where they have been assigned a considerable older (Late Cenomanian) age (Fig. 3). As a consequence, these sediments are here designated as "Rivas transitional deposits" and assigned a Late Cretaceous age.

The rocks underlying the Rivas Formation are not exposed, but are assumed to consist of pelagic sediments or oceanic crust with affinities to the Nicoya Complex (cf. Dengo, 1962) together with organic-rich cherts and shales of the Loma Chumico Formation (cf. Astorga, 1987). The Nicoya Complex is regarded as Jurassic to Late Cretaceous in age and is composed mainly of basalts derived from primitive island-arc and oceanic crust, mixed with small amounts of intra-arc and fore-arc volcaniclastic and sedimentary rocks (Gursky and Schmidt-Effing, 1983; Bourgois *et al*., 1984; Astorga, 1987; Lundberg, 1991; Frisch *et al*., 1992). The Complex is present in the subsurface of the Tempisque Basin (Fig.1B; Galli-Olivier, 1979; Frisch *et al*., 1992) and can be studied at outcrop in the Nicoya Peninsula in NW Costa Rica. In Nicaragua, the Complex only outcrops at one location on the eastern margin of the Sandino Basin at the San Juan River at Sábalos (Fig.1B). In the subsurface, basaltic rocks and related pelagic sediments have been recorded at onshore wells *Rivas-1* and *El Ostional-1* which are located on the southern margin of the Sandino Basin (Figs. 1B and 3).

The Nicoya Complex is overlain by a series of interbedded organic-rich cherts and shales, defined as the Loma Chumico Formation (cf. Astorga, 1987), which represents an important source rock interval within the forearc basins of western Costa Rica (*see below*). Age determinations for the Loma Chumico Formation range widely from the Early to Late Cretaceous — Aptian to Early Campanian (Astorga, 1988; 1990) or, alternatively, late Cenomanian to Campanian (Erlich *et al*., 1996). The deposition of organic-rich intervals has been correlated with ocean-wide anoxic events during Aptian-Albian and Cenomanian/Turonian (Astorga, 1988, 1990, 1994; Astorga *et al*., 1991). The Loma Chumico Formation is therefore here assigned an Albian age.

The Loma Chumico Formation is conformably overlain by cherts and siliceous limestones of the Sabana Grande Formation (cf. MacDonald, 1920), which is well known from the adjacent Tempisque Basin of NW Costa Rica (Fig. 1B, e.g. Lundberg, 1991). In the *Rivas-1* and *El Ostional-1* wells, limestones have been encountered that have been correlated to this formation and were originally assigned a Cenomanian age (Fig. 3). Normally, the Sabana Grande Formation is described as Senonian (Dengo, 1962) or Campanian (Galli-Olivier and Schmidt-Effing, 1977; Baumgartner *et al*., 1984; Lundberg, 1991). The formation is generally thought to reflect the first subaerial emergence of the ancestral Costa Rican island-arc, which is dated as Late Campanian (Schmidt-Effing, 1979; Lundberg, 1982; 1991; Gursky and Schmidt-Effing, 1983; Astorga *et al*.,1991; Seyfried *et al*.,1991; Winsemann and Seyfried, 1991). According to data from wells *Rivas-1* and *El Ostional-1*, a Cenomanian limestone was tentatively included into the "Sabana Grande" Formation in this study, although the authors are aware of discrepancies with the existing literature.

The Sabande Grande is overlain by the Rivas Formation whose upper boundary onshore is picked at the base of the basal conglomerate of the overlying Brito Formation (cf. Hayes, 1899, cited in Hoffstetter *et al*., 1960) indicating a depositional hiatus in the Paleocene between these two formations (Wilson and Fagginger, 1942; Zoppis and Del Guidice, 1958; Kuang, 1971). However, further investigations demonstrated the occurrence of similar sediments during Paleocene times and therefore extended the age of the Rivas Formation to the Late Palaeocene (e.g. Astorga, 1987; 1988). This is also supported by the interpretation of reprocessed seismic data (Ranero *et al*., 2000b), which indicate continued sedimentation throughout the Palaeocene. The Brito Formation is characterised by claystones, siltstones and sandstones with a high content of feldspars and volcanic material; partly silicified limestones also occur (e.g. Astorga, 1987, 1988; Winsemann, 1992). In addition, Middle Eocene hemipelagic shales have been mapped onshore which are rich in organic matter ("black shales") and represent a potential source rock interval (Darce *et al*., 2000 b; *see below*).

The Brito Formation crops out along the Pacific coast of SW Nicaragua and NW Costa Rica where it is interpreted to represent stacked channel-levee deposits of small-scale radial, overlapping submarine fans (Winsemann and Seyfried, 1991; Winsemann, 1992; Struss *et al*., 2007). The age of the coastal succession was originally described by Hayes (1899) as Late Cretaceous to Early Oligocene, but later results from biostratigraphic analyses indicated a Middle to Upper Eocene age (Baumgartner *et al*., 1984; Winsemann, 1992). In the subsurface, the Brito Formation has been penetrated by wells *Corvina-2* (offshore) and *El Ostional-1* (onshore), the latter suggesting a latest Paleocene to Early Oligocene age (Fig. 3). Based on offshore seismic data, Ranero *et al.* (2000b) described sedimentation continuing during the Late Eocene to Early Oligocene in the area of the deep basin and platform (Fig. 2) and correlated it to the Brito Formation.

The Brito Formation is unconformably overlain by Late Oligocene to Early Miocene volcaniclastics of the Masachapa Formation (cf. Wilson, 1941, cited in Hoffstetter *et al*., 1960). Offshore, the formation is present in all four wells (Fig. 3). It is composed of tuffaceous shales interbedded with siltstones and sandstones which are dominant in the upper part of the section. Onshore investigations on behalf of the INE suggested a deep-marine environment for the lower part with a transition into shallow-water deposits of generally minor thickness and extent in

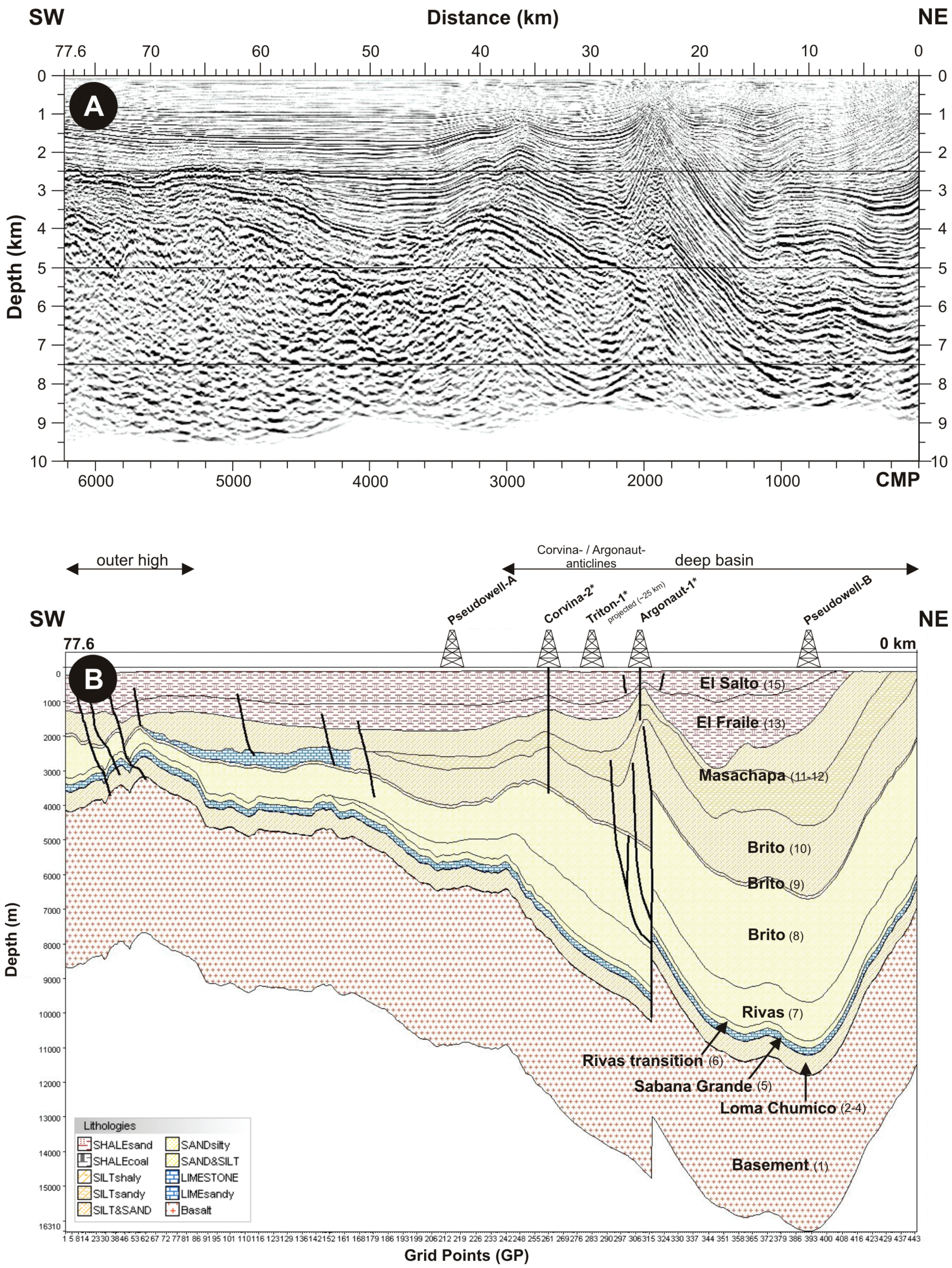

Fig. 2A. NE-SW regional 2D seismic section across the offshore Sandino Basin (reproduced by permission of C. Ranero and IFM-GEOMAR). The main elements of the section are the deep basin in the NE, the Argonaut anticline with a prominent flower structure in the centre, and the outer structural high in the SW.
(B) Interpreted cross section along the seismic line. For input parameters, see Table 3. Ages are based on wells *El Ostional-1* and *Rivas-1* for the Cretaceous to Lower Paleogene, and wells *Corvina-2* and *Argonaut-1* for the Middle Paleogene to Neogene; the lithologies are consistent with well information summarized in Fig. 3. See Fig. 1b for well locations.

its upper part. Unlike the submarine fan deposits of the underlying Brito Formation, Struss *et al. (in press*) describe the Masachapa Formation as mainly consisting of small, isolated channels and gullies filled with sandstones and conglomerates which are incised into laterally extensive mudstone to sandstone successions of a deep-marine slope environment.

The deep-marine succession is unconformably overlain by shallow-water and continental pyroclastic deposits of Middle Miocene to Pleistocene age (Kolb and Schmidt, 1991; Krawinkel and Kolb, 1994), which have been drilled by all four offshore wells (Fig. 3).

The Middle to Late Miocene El Fraile Formation (cf. Wilson, 1941; Kolb and Schmidt, 1991) consists of calcareous sandstones, siltstones, shaly tuffs and tuffs, conglomerates and volcaniclastic breccias, which were deposited within shoreface-shelf, estuarine-deltaic and alluvial systems. In the NE of the Sandino Basin, these sediments laterally interfinger (Weyl, 1980) with continental deposits of the Tamarindo Formation (cf. Wilson, 1941; Kolb and Schmidt, 1991; Krawinkel and Kolb, 1994).

The El Fraile Formation is overlain by the Pliocene El Salto Formation (cf. Wilson, 1941; Kolb and Schmidt, 1991) deposited within a beach and lagoonal or marginal bay environment. It is dominated by mixed carbonate-siliciclastics consisting of calcarenites, marls, and clastic or detrital fossiliferous limestones (coquinas and oyster reefs) (Kolb, 1990; Kolb and Schmidt, 1991). Offshore, the El Salto Formation gently onlaps onto sediments of the El Fraile Formation suggesting a hiatus in sedimentation (Ranero *et al*., 2000 b). The Neogene shallow-water sediments of the El Fraile and El Salto Formations are drilled in the offshore wells *Corvina-1* and *Corvina-2, Argonaut-1* and *Triton-1* (Fig. 3).

SOURCE AND RESERVOIR ROCKS

Regional source rocks include the black shales of the Cretaceous Loma Chumico Formation which is known in the adjacent Tempisque Basin of NW Costa Rica (Astorga, 1988, 1990). Age determinations for this formation range widely between the Aptian to Campanian (Astorga, 1988; 1990; Erlich *et al*., 1996). Based on the occurrence of Cretaceous sediments similar to the Loma Chumico Formation, which were encountered in the onshore *Rivas-1* and *El Ostional-1* wells, this formation is inferred to be present overlying basement rocks in the Sandino Basin (Fig. 3; Darce *et al*., 2000b; Ranero *et al.*, 2000b).

Samples from the Santa Elena Peninsula in NW Costa Rica (Fig. 1B) contained Types I and II kerogen with a total organic carbon (TOC) content ranging between 4.4 and 54.8 % and an average of 10 % (Astorga, 1997; Darce *et al*., 2000 b). The deposition of these organic-rich rocks may be associated with ocean-wide Cretaceous anoxic events (e.g. Astorga, 1988; 1990; 1994; Astorga *et al*., 1991) or the upwelling of nutrient and silica-laden waters in the area of the ancestral Costa Rican island arc (Erlich *et al*., 1996).

A second potential source rock in the Sandino Basin is constituted by Middle Eocene black shales of the Brito Formation. Weathered outcrop samples of these shales have TOC values of 0.29-0.95 %, and the TOC content of unweathered samples is predicted to be up to 2.0 % (Darce *et al*., 2000 b). Organic matter is terrestrial Type III kerogen (Darce *et al*., 2000 b). For oil-source rock correlation, an oil sample from the seep at the Citalapa River was analysed on behalf of INE. The oil has an API gravity of 12.6°. Column chromatography revealed that the oil is severely to extremely biodegraded. Gas chromatography-mass spectrometry (GC/MS) indicates that the remaining biomarkers are dominated by the compound oleanane. This suggests that the source rock for the oil contained abundant higher plant material. Several samples from the Brito Formation contain this compound and accordingly are considered as candidate source rock for the oil seep.

Potential reservoir rocks are expected to be present at both at both the outer structural high and in the region around the Corvina anticline (Fig. 2). High amplitude, high-velocity layers on the inner flank of the outer structural high are interpreted as carbonate ramps and reefs, respectively (Ranero *et al*. 2000b); these have also been reported from an analogous location in Costa Rica (Seyfried *et al*., 1991; Calvo, 2003). Sand-rich packages which are frequently interbedded within the basin's sedimentary succession may serve as reservoir rocks. Deep-water sandstones of the Brito and Masachapa Formations as well as shallow-water sandstones of the El Fraile Formation represent potential reservoirs. Petrographic analyses of outcrop samples by INE *(unpublished*) recognised two main types of sandstones with somewhat varying compositions throughout the stratigraphic column: greywackes and arenites. Thus, the normative quartz content increased upwards from less than 5 % in the sandstones of the Rivas Formation to about 30 % in the El Fraile Formation. The proportion of lithoclasts of igneous rocks, such as diorites, also increased upwards reaching higher percentages in the Masachapa and El Fraile Formations. Diagenetic alterations resulting in partial occlusion of the primary porosity downgrades the general reservoir potential of the basin. The initial porosity of e.g. litho-feldspathic arenites is partially filled by secondary clay matrix (on average 15-25 %), which originated from the alteration of feldspathic and volcanic lithoclasts. Early diagenetic calcitic cements (on

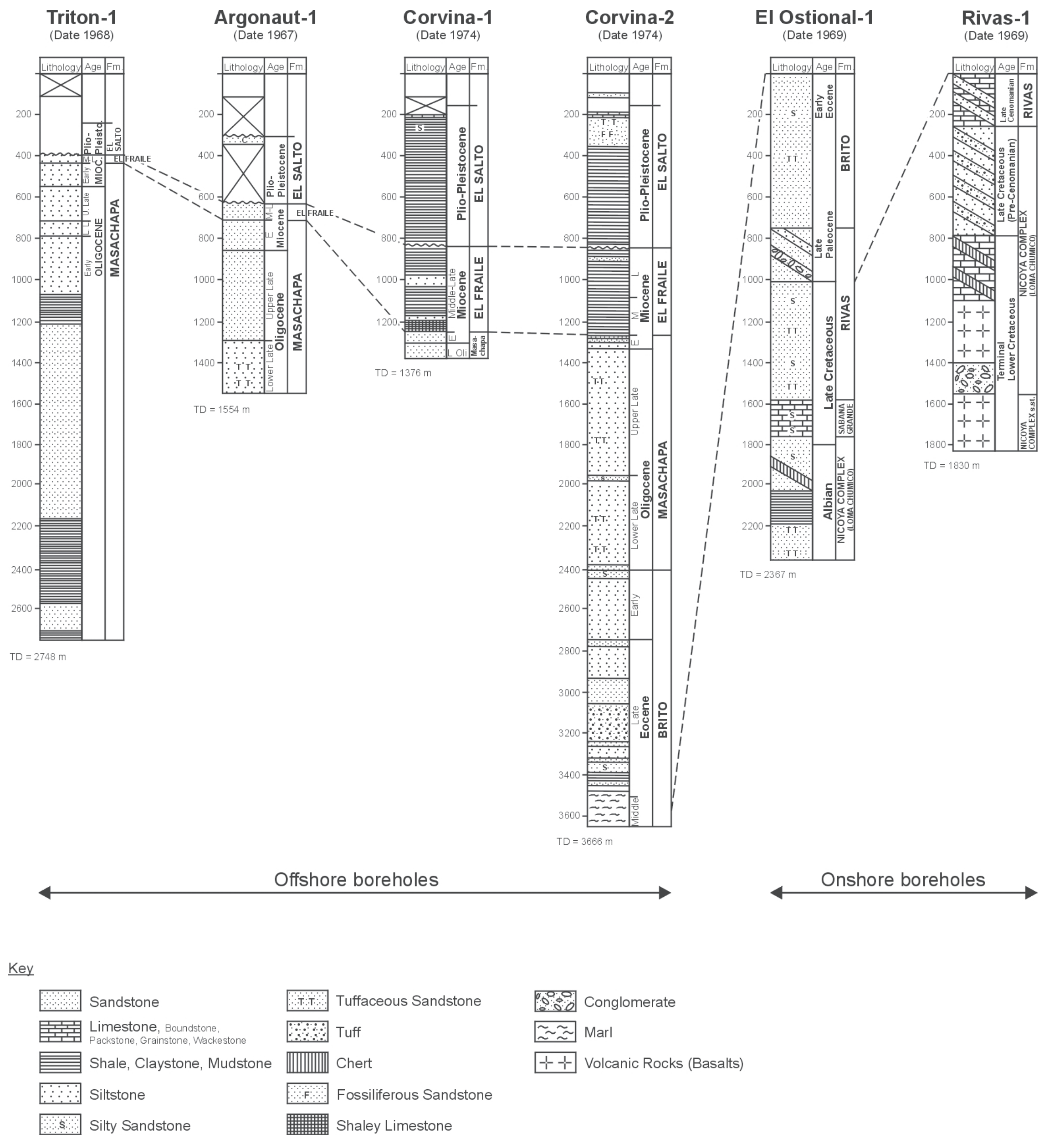

Fig. 3. Correlation of wells in the Sandino Basin. Wells *Corvina-2* and *Argonaut-1* are located on the studied seismic section and were used for lithology and age assignments; the *Triton-1* and *Corvina-1* boreholes are located nearby. The onshore boreholes *El Ostional-1* and *Rivas-1* provide information about the Paleocene to Cretaceous sedimentary sequence. Data compiled from INE internal reports and Ranero *et al.* (2000b).

average 10-15 %) and local siliceous and ferric cements (<5 %) are also important.

However, the presence of potential stratigraphic traps in the Brito, Masachapa and El Fraile Formations might be favoured by the generally higher proportion of mature quartz-rich sandstones in the upper parts of the succession, and the development of secondary porosity due to late diagenetic dissolution of feldspars and fracturing. For example, samples from the deep-water sandstones of the Brito Formation at the recently-drilled onshore wildcat *San Bartolo Rodriguez Cano-1* had porosities of 17-21 % and permeabilites of 3-30 mD (IHS, 2007). In addition, porosities of 16-24 % and permeabilities of 2-75 mD have been reported from the onshore well *Las Mesas Gutierrez-1* which is located 11 km west of *San Bartolo-1**.

Recent onshore field studies of the Brito and Masachapa Formations have drawn attention to numerous thicker-bedded and coarse-grained sandstone bodies which may form analogues for subsurface exploration targets. These sandstone bodies are interpreted to represent deep-water channel fills and to form parts of relatively small, radial submarine fans (Brito Formation) or to

* see http://www.norwoodresources.com/s/Home.asp).

represent small, isolated channels and gullies that were deposited within a deep-water slope environment (Masachapa Formation), respectively (Winsemann, 1992; Struss *et al*., 2007; *in press*). The channels cut into finer-grained deposits which have sealing potential. Such facies changes, resulting in vertical and lateral interfingering of sandy and shaly units, may have led to the development of stratigraphic traps. Structural traps may be associated with the outer high and the anticlines in the central Sandino Basin (Darce *et al*., 2000b). Tertiary shales acting as a seal are known from exploration wells and are inferred to occur over large areas both on- and offshore Nicaragua.

MATERIALS AND METHODS

To evaluate the quantity, quality and maturity of organic matter along the 2D seismic line, the organic geochemistry of 63 cuttings samples from well *Corvina-2* (Figs. 1B, 2) was investigated at the laboratories of the Federal Institute for Geosciences and Natural Resources (BGR), Germany. Samples were provided by INE. No cores from the offshore part of the Sandino Basin are currently available. Thus cuttings samples from well *Corvina-2* provided the only method of directly evaluating the source rock potential of the Tertiary succession. Analyses included the determination of total organic carbon content (TOC), the measurement of vitrinite reflectance, and Rock-Eval pyrolysis.

To prepare the cuttings for TOC and Rock-Eval analysis, samples were solvent-washed to remove contamination by oil-based drilling mud. Extraction was carried out using a dichloromethane solvent. The TOC of the 63 cuttings samples was measured on a *LECO CS-200* instrument and is expressed in weight percent (wt %). Aliquots of crushed samples were weighed into ceramic crucibles and decarbonised with 2N hydrochloric acid (HCL) by heating to 60°C. After decarbonatisation, samples were washed with distilled water to remove the HCL and water-soluble chlorides. The samples were combusted in an induction oven at 2000°C in an oxygen atmosphere, and the amount of CO_2 generated during combustion was recorded.

Rock-Eval pyrolysis (Espitalié *et al*., 1977; Radke *et al*., 1997) was performed on a *Rock-Eval 6* instrument (Vinci Technologies). Results included Tmax (°C), hydrogen index HI (mgHC/gTOC) and the oxygen index, OI (mgCO_2/gTOC). The cuttings samples were pulverised and weighed as aliquots into ceramic crucibles. During pyrolysis, the powdered samples were heated under an inert gas flow and the released hydrocarbons were quantified as a function of temperature. The samples were first heated at 300°C for three minutes. The recorded S1 peak during this phase represents the amount (in mg) of free and adsorbed hydrocarbons that can be thermally distilled from one gram of rock (mg HC/g rock). In a second step, the sample was heated at a linear temperature gradient of 25°C/min to 650°C for 14 min. The recorded S2 peak reflects the amount (in mg) of hydrocarbons generated by pyrolysis of the kerogen in one gram of rock (mg HC/g rock). Tmax (°C) corresponds to the temperature at which maximum hydrocarbon generation occurs and can be used as a maturity indicator. The S3 peak represents the CO_2 generated during combustion and is expressed in mg CO_2/g rock. The hydrogen index (HI) is a measure of the remaining hydrocarbon generation capacity, and corresponds to the quantity of pyrolysable hydrocarbons from S2 per unit TOC (mg HC/g Corg). The oxygen index is the normalized amount of CO_2 produced during pyrolysis (mg CO_2/g Corg).

Petroleum generation in the Sandino Basin was modelled on the basis of sample-specific reaction kinetic parameters. The standard temperature programme of the *Rock-Eval 6* device was used as previously described. Five cuttings samples of potential source rocks from the Masachapa and Brito Formations were pyrolysed at heating rates of 1 K/min (max. 446 min), 5 K/min (c. 99 min), 10 K/min (c. 50 min) and 25 K/min (c. 20 min) in order to investigate the timing of oil and gas generation.

Random vitrinite reflectance (Rr %) was measured on 39 selected cuttings samples from well *Corvina-2*, of which 15 samples gave useful data. Measurements followed standard methods (e.g. Taylor *et al*., 1998). The samples were crushed and mounted in synthetic resin, and the solid plugs were polished to a thickness of <1 mm. Vitrinite reflectance was measured on randomly oriented vitrinite grains with a *Leica* microscope (X500) under oil immersion at a wavelength of 546 nm (using polarised light). Vitrinite macerals were observed under fluorescence (excitation by blue light).

RESULTS

Quantity and type of organic matter

Cuttings samples from well *Corvina-2* varied in grain-size from mudstones to sandstones. Table 1 presents organic geochemical data for the samples analysed. TOC values vary between 0.16 % for the Plio-Pleistocene El Salto Formation and 3.16 % for the Late Oligocene to Early Miocene Masachapa Formation. Maximum TOC values for the Middle to Late Miocene El Fraile Formation (2.2 %), the Late Oligocene to Early Miocene Masachapa Formation (3.2 %), and the Eocene to Early Oligocene sediments of the Brito Formation (1.9 %) indicate that these units may have some source rock potential.

Formation	Depth below sea floor (m)*	TOC (wt %)	HI (mg_{HC}/g_{TOC})	OI (mg_{CO2}/g_{TOC})	T_{max} (°C)	Vitrinite Reflectance (R_r %)
El Salto	228	0.43	33	577	413	
	320	0.47	60	851	399	0.42
	356	0.53	58	489	416	0.30
	402	0.50	56	612	415	
	457	0.62	58	529	415	
	503	0.55	89	620	392	
	548	0.49	71	555	388	
	640	0.73	74	341	398	
	685	1.17	108	252	415	
	731	1.86	151	182	422	0.35
	759	1.59	103	278	421	0.36
	777	1.94	111	248	421	
El Fraile	832	1.51	101	319	422	
	878	1.53	94	286	420	0.25
	914	1.28	77	286	420	
	1024	1.25	68	315	416	
	1060	1.08	55	327	410	
	1097	1.20	63	312	413	
	1134	1.12	111	247	417	
	1189	2.20	152	192	419	0.36
	1234	1.08	54	367	410	
	1280	0.58	52	386	404	
Masachapa	1335	0.91	105	213	424	
	1379	1.14	115	151	418	
	1443	1.41	182	133	430	
	1498	1.42	208	150	433	
	1544	1.69	212	206	435	
	1589	1.90	233	154	427	
	1635	1.36	154	129	425	
	1690	1.70	197	159	432	
	1736	2.05	247	118	430	
	1873	3.16	351	98	429	0.34
	1919	3.01	268	92	428	0.32
	1964	1.84	184	111	430	
	2019	1.27	161	149	433	
	2083	1.65	201	108	437	
	2129	1.67	235	111	431	0.38
	2184	1.26	188	140	434	
	2257	1.08	169	145	433	0.33
	2312	1.07	172	132	432	0.45
	2358	1.04	125	139	433	
Brito	2413	1.34	218	127	433	
	2477	1.05	102	153	429	
	2532	1.02	150	166	434	
	2614	1.53	171	114	431	
	2660	1.39	191	106	433	
	2714	1.52	252	103	436	0.29
	2769	1.07	164	124	437	
	2815	1.14	109	139	428	
	2870	1.06	177	126	431	
	2916	1.00	206	145	433	
	2989	0.89	219	138	432	0.33
	3044	0.85	235	166	439	
	3117	1.12	278	123	432	0.39
	3172	0.99	240	188	435	
	3263	0.92	253	163	422	
	3318	0.80	270	171	427	
	3382	0.99	409	161	434	
	3428	1.49	428	123	430	
	3474	1.17	376	143	438	
	3528	1.28	484	134	438	
	3592	1.88	414	104	446	0.40
	3638	1.82	396	147	447	

- Depth from the middle of the sampled interval.

Table 1. Results of TOC, Rock-Eval and vitrinite reflectance measurements of solvent-washed cuttings samples (well *Corvina-2*).

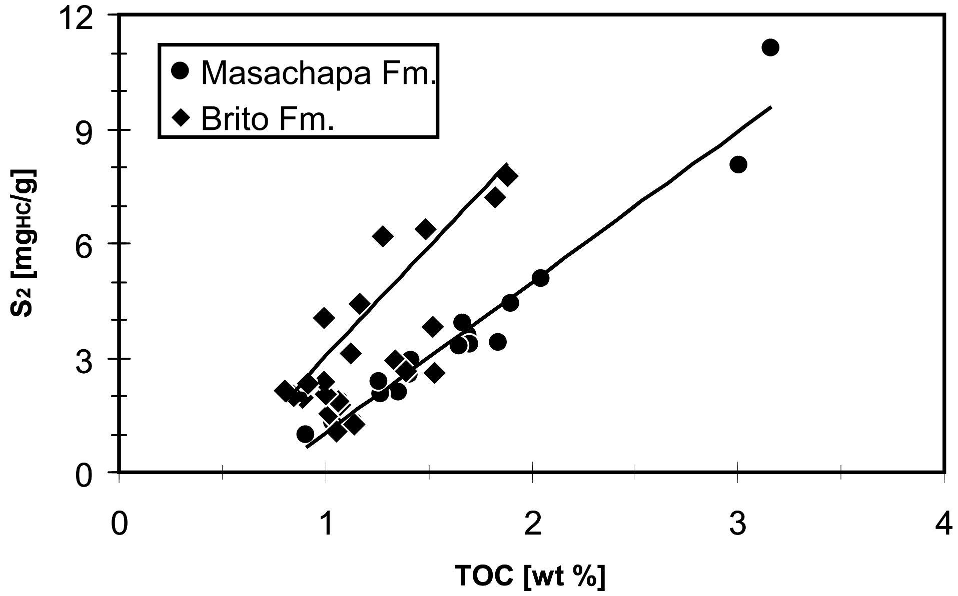

Fig. 4. Cross-plot of S2 versus TOC of samples from the Brito and Masachapa Formations with calculated linear regressions (after Langford and Blanc-Valleron, 1990). Brito Formation: $y = -2.751 + 5.771x$ ($r^2 = 0.89$). Masachapa Formation: $y = -2.929 + 3.954x$ ($r^2 = 0.95$).

Measured hydrogen indices (HI) at well *Corvina-2* range between 33 and 484 mg HC/g TOC, reaching a maximum for samples of the Brito Formation below 3428 m. A plot of S2 versus TOC (Fig. 4) indicates differences between the Masachapa and Brito Formations, because data-points appear to fall on different trend lines suggesting differences in organic matter composition. An average hydrogen index can be approximated by calculating the slope of the S2 versus TOC regression line (Langford and Blanc-Valleron, 1990). HI values thus calculated are 395 mg HC/g TOC for the Masachapa Formation and 577 mg HC/g TOC for the Brito Formation, respectively. Oxygen indices of cuttings samples over a depth range of 832 m to 3638 m show values between 92 and 386 mg CO_2/g TOC. Samples of the Plio-Pleistocene El Salto Formation have oxygen indices of up to 851 mg CO_2/g TOC.

Fig. 5 shows a plot of hydrogen index versus oxygen index and Tmax. This diagram indicates that the organic matter in the samples of the Masachapa and Brito Formation can be classified as mixed Type II-III kerogen, with some potential to generate oil and gas (cf. Peters, 1986). However, rocks of the Brito Formation contain more hydrogen-rich kerogen pointing to a generally higher oil-generating potential. Organic matter in the El Salto and El Fraile Formations can be classified as predominantly Type III kerogen.

Maturity

Tmax values range from 388 to 447°C (Table 1), with most values below 435°C in samples from Oligocene to Plio-Pleistocene formations indicating thermal immaturity (cf. Espitalié, 1986; Peters and Cassa, 1994). The highest Tmax values were reached within the lowermost part of the succession from well *Corvina-2* in samples of the Brito Formation, indicating thermal maturity at depths below 3,400 m.

Optical analysis showed the presence of vitrinite macerals and some liptinitic grains within cuttings samples from the Masachapa and Brito Formations, confirming the mixed terrestrial and marine origin of the organic matter. In the majority of cases, vitrinite grains were too small for an accurate determination of reflectance to be made. Therefore, only a small number of measurements could be made for each sample leading to a comparatively large error (± 0.05 % Rr). Measured vitrinite reflectance values range between 0.25 and 0.45 % Rr, and indicate that the organic matter is immature with respect to petroleum generation (Table 1).

In summary, the geochemical evaluation of cuttings samples from well *Corvina-2* indicate that sediments of the Masachapa and Brito Formations are sufficiently rich in organic matter and have an appropriate kerogen content to have some potential for petroleum generation and expulsion. However, Tmax values and vitrinite reflectance data indicate a low level of thermal maturity at this location.

Petroleum generation kinetics

Petroleum generation from the investigated source rocks is shown for a heating rate of 25 K/min in Fig. 6. From these results, kinetic parameters such as activation energy distribution, frequency factors and generation potential were determined using *Pyrocalc*,

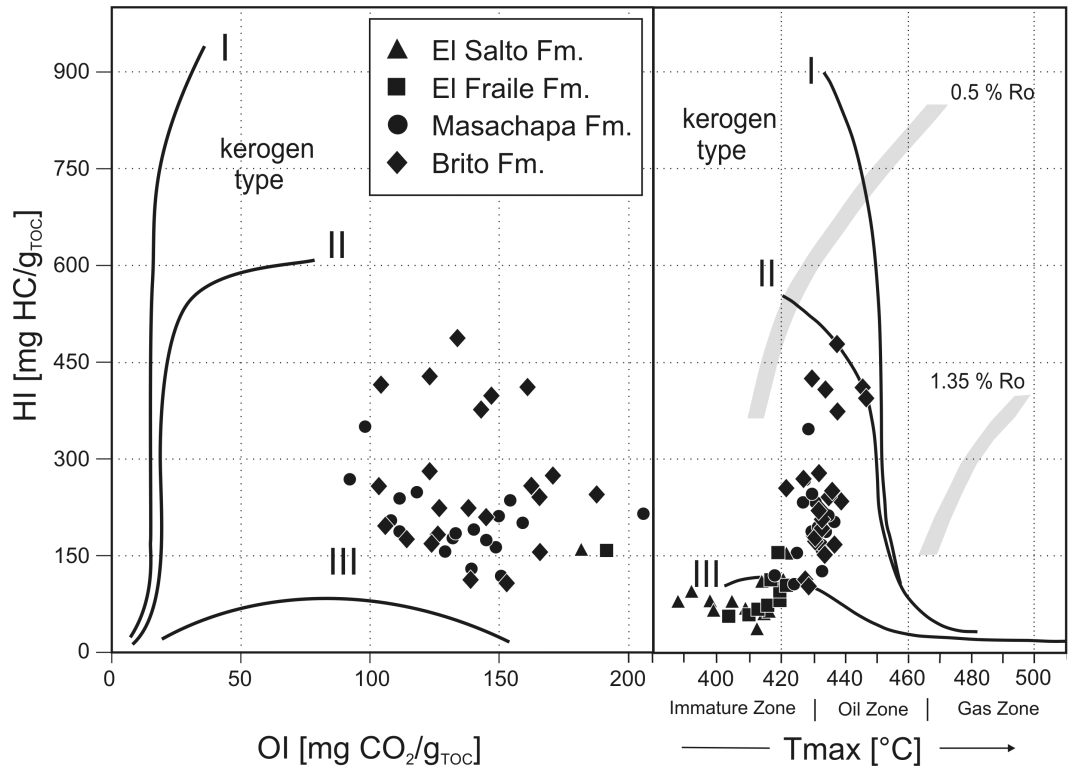

Fig. 5. Cross-plot of hydrogen index (HI) versus oxygen index (OI) and plot of HI versus Tmax with fields of kerogen type and maturity (after Espitalié, *et al.*, 1986).

Formation	Depth below Sea Floor (m)	Stratigraphy	Vitrinite Reflectance (R_r %)	TOC (wt %)	HI (mg_{HC}/g_{TOC})	Activation Energy (kcal/mol) of Maximum Initial Petroleum Potential	Range of Activation Energies (kcal/mol)	Frequency Factor (Ma-1)
Masachapa	1873	Upper Oligocene	0.34	3.16	351	46	28-60	2.0E+025
Brito	3428	Upper Eocene	n/a	1.49	428	48	28-58	4.0E+025
Brito	3592	Middle Eocene	0.40	1.88	414	50	28-64	1.6E+026

Table 2. Kinetic analysis of bulk Rock-Eval results from selected samples from well *Corvina-2* processed with *Pyrocalc* software (n/a: not available).

and results are summarized in Table 2. The three analysed samples are characterised by relatively high hydrogen indices (351-428 mg HC/g TOC). All samples show a wide distribution of activation energies with equally high Arrhenius factors. On the basis of their geochemistry (HI, OI, Tmax), the three samples were classified as containing mixed Type II-III kerogen. As a consequence, differences between the kinetic parameters of the individual samples are relatively small. Individual kinetic models obtained with *Pyrocalc* were integrated into a basin modelling study (*see below*).

2D BASIN MODELLING

Numerical basin modelling was performed using *PetroMod 8*. For modelling purposes, data from seismic, stratigraphic and geological interpretations

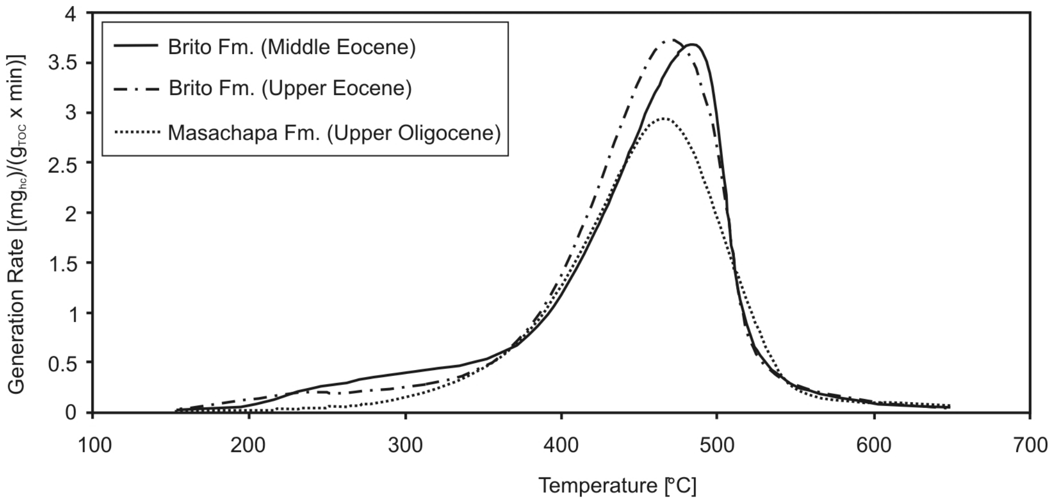

Fig. 6. Generation rate of three source rock samples from the Brito and Masachapa Formation calculated with a heating rate of 25K/min.

were combined with information about the structural evolution of the basin, its palaeobathymetry and palaeo heat-flow characteristics, and organic geochemistry. A finite-element grid was constructed based on a NE-SW trending reflection seismic line, some 78 km long (Figs. 1, 2). The seismic line was divided laterally into 444 gridpoints and vertically into 16 discrete intervals of sedimentation, non-deposition or erosion of specified ages and durations using the chronological chart of Haq *et al.* (1987). The deepest part of the basin including the Loma Chumico, Sabana Grande, Rivas and parts of the Brito Formation extends below the seismic data record and had to be inferred for the conceptual basin model. Reconstruction of the burial history of the basin shows that this area remained relatively unaffected by structural modification during deposition of these formations (*see below*). We therefore assumed laterally continuous thicknesses. For the conceptual model, eleven different lithologies were assigned to the individual layers according to the standards given in *PetroMod* (Fig. 2; Table 3).

The seismic line crosses the offshore wells *Corvina-2* and *Argonaut-1*. *Corvina-2* is the deepest well in the offshore sector of the Sandino Basin and bottomed in Middle Eocene sediments of the Brito Formation (Fig. 3). From this well, it became evident that the generally poor biostratigraphic control can result in different interpretations of the stratigraphic succession (Fig. 7). However, the most recent stratigraphic analysis conducted on samples from *Corvina-2* (*sensu* Steinsberg, 1980) led to a fundamental change in the interpretation of the Miocene and Oligocene sequences (see Fig. 7). Up to now, a single stratigraphic model for the Sandino Basin has not been accepted, and this seriously hampers the reconstruction of the burial and temperature histories of the basin. Therefore, the most recently published well interpretation (Ranero *et al.*, 2000b) was adopted to assign the ages in the conceptual model.

For modelling the burial history, palaeobathymetric data from INE well reports were used. These data indicate an overall shallowing in water depths from abyssal to neritic conditions since Cretacous times.

For the reconstruction of the thermal history the temperature distribution within the sediments over time was determined using *PetroMod*, taking into account the basal heat flow, the thermal conductivities of the rocks and the surface temperature. The sediment-water interface temperature (SWIT), the upper boundary condition for heat transport in the basin, was available from latitude-dependent diagrams of ocean surface temperatures (Wygrala, 1989). The amount of heat entering the basin at the base was calibrated using measured vitrinite reflectance data from well *Corvina-2* (Fig. 8; Table 1).

Burial and thermal history

Ranero *et al.* (2000b) applied backstripping techniques to the seismic line presented in this paper, and interpreted the basin evolution as follows:

As a consequence of the subduction of the Farallón Plate beneath the Caribbean Plate in the Late Cretaceous, basin development began near the present-day coastline. The pinch-out of the Rivas Formation (Fig. 9A) against the western flank of the basin, and the seaward thinning of the Brito Formation (Fig. 9B) indicate the presence of a deep basin and a "topographic barrier" near the present-day outer structural high from Late Cretaceous to Paleocene time (Ranero *et al.*, 2000b). In the Eocene and Oligocene, during deposition of the Brito and Masachapa Formation, the central part of the basin subsided (Fig. 9B, C). As a result, the upper part of the Brito Formation as well as the lower Masachapa Formation pinches out against the outer high. The

Event -No.	Age [Ma]	Interval	Thickness [m]			Lithology	PSE	HI [mg/gHC]/TOC [%]/ Kerogen Type	PWD* [m]	SWI* [° C]
			GP 215	GP 263	GP 392					
15	5.5	El Salto Fm.	1015	777	404	SHALEsand	Overburden Rock		30	22
14	5.8	Hiatus							40	22
13	16.5	El Fraile Fm.	786	404 (- 53)	1210 (- 113)	SHALEsand	Reservoir Rock		400	13
12	28.4	Masachapa Fm.	761	745 (- 106)	1640	SILT&SAND	Source Rock	395.4/1.8/II-III	1500	8
11	30	Masachapa Fm.	371	448	1367	SILTsand	Source Rock	395.4/1.29/II-III	2000	9
10	39.5	Brito Fm.	1049	1133	2041	SILT&SAND&LIMESTONE	Source Rock	428/1.12/II-III	3000	10
9	39.6	Brito Fm.	90	90	90	SILTshaly	Source Rock	314.7/1.66/II-III	3000	10
8	58.5	Brito Fm.	1006	2170	2989	SANDsilt	Reservoir Rock		3000	14
7	68.5	Rivas Fm.	364	1271	1124	SANDsilt			3000	15
6	93.5	Rivas Fm. Transition?	200	200	200	SAND&SILT			3000	15
5	96.5	Sabana Grande Fm.	200	200	200	LIMESTONEsand	Reservoir Rock		3000	15
4	98.5	Loma Chumico Fm.	15	15	15	SHALEcoal	Source Rock	500/10/II	3000	15
3	107	Loma Chumico Fm.	570	570	570	SILT&SAND			3000	17
2	108	Loma Chumico Fm.	15	15	15	SHALEcoal	Source Rock	500/10/II	3000	17
1	113	Basement	4500	4500	4500	BASALT			3000	17

- PWD = paleowater depth; SWI = sediment-water interface temperature

Table 3. Input parameters of the basin model at Grid Points (GPs) 215, 263 and 392 (for locations, see Fig. 2B).

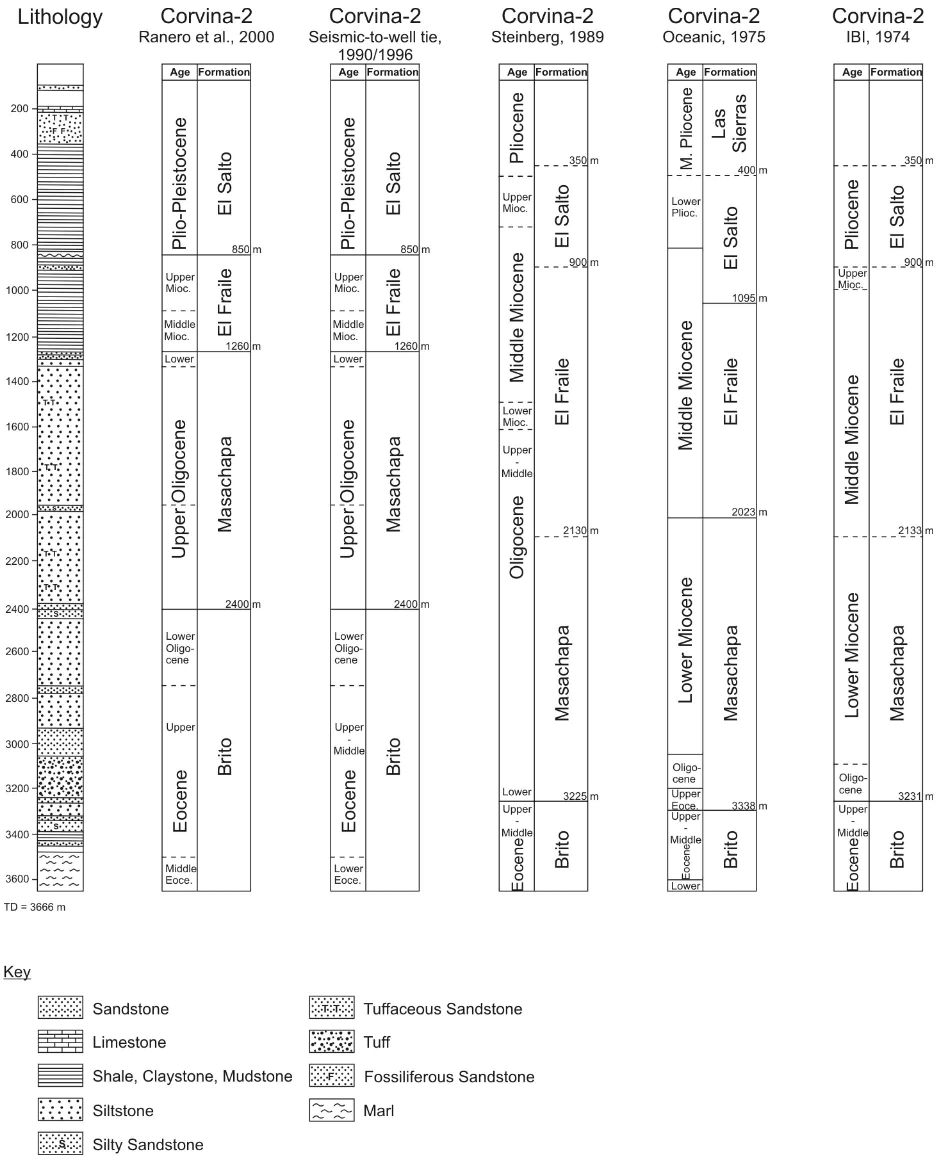

Fig. 7. Stratigraphic colums for the *Corvina-2* borehole summarizing the results of different investigations made since 1974 (modified from INE internal reports). For basin modelling, the stratigraphic interpretation of Ranero *et al*. (2000b) was used.

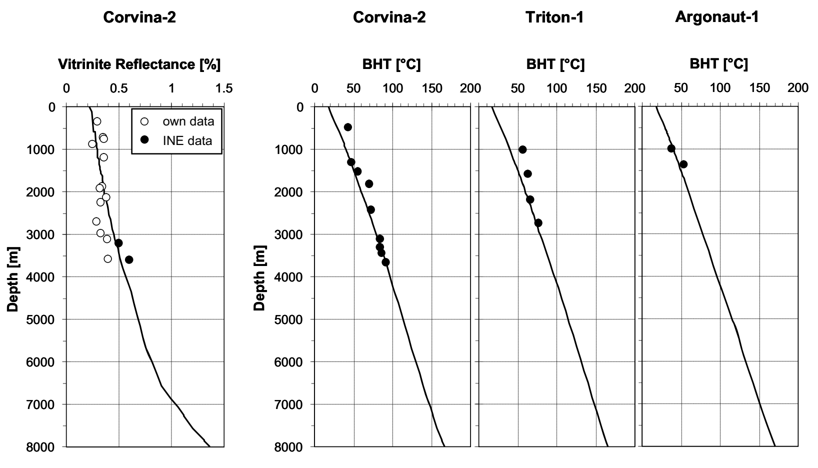

Fig. 8. Bottom-hole temperatures (BHT) and vitrinite reflectance profiles versus depth for calibration of the basin model. Trends were modelled using the EASY%Ro algorithm of Sweeney and Burnham (1990). Data derived from the Instituto Nicaragüense de Energía (INE) are shown as black dots.

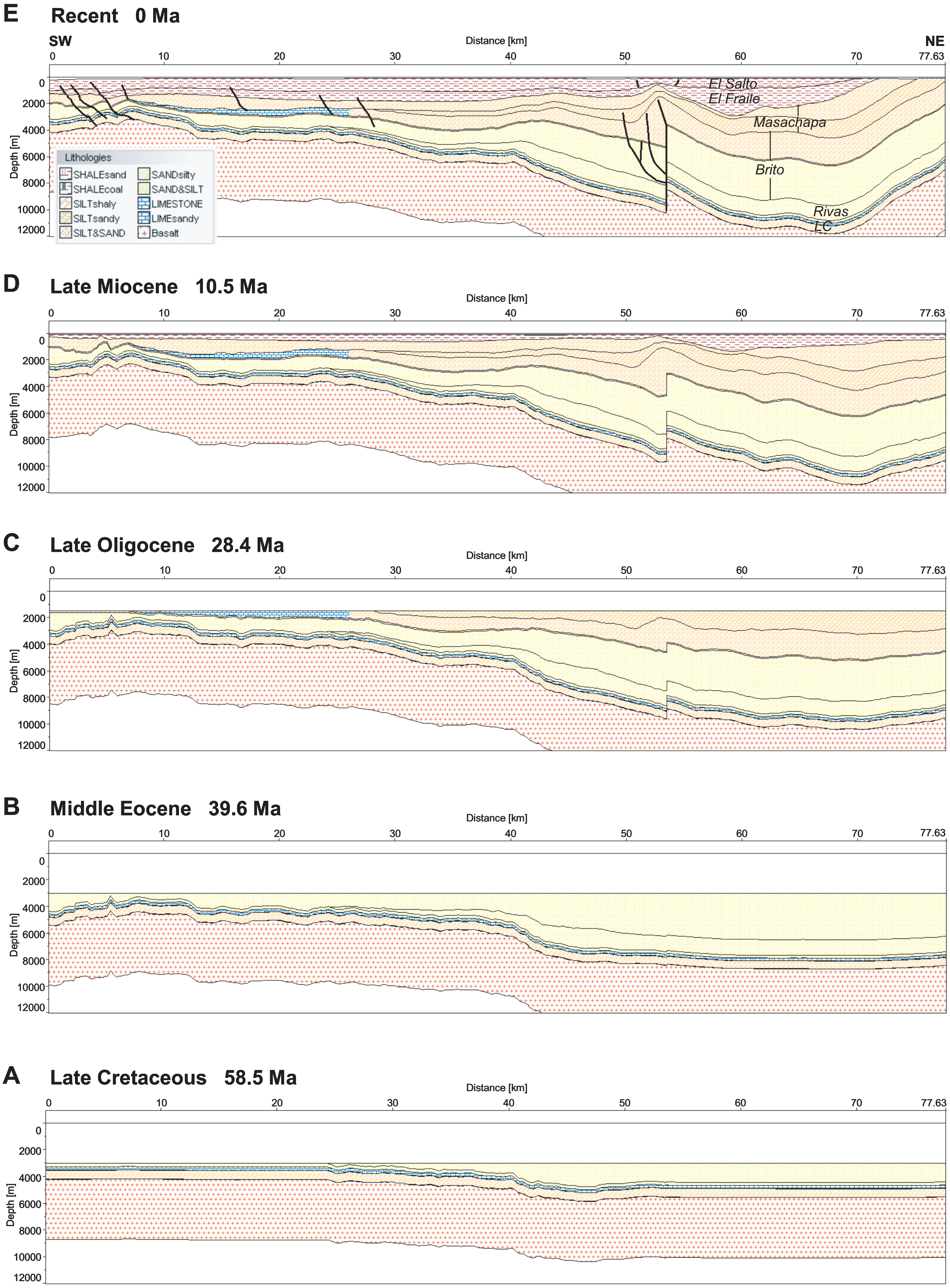

Fig. 9. Reconstructed structural development of the Sandino Basin along the modelled section for: A. the Late Cretaceous; B. the Middle Eocene; C. the Late Oligocene; D. the Late Miocene; and E. the present day (Recent). Lithologies are based on well information shown in Fig. 3.

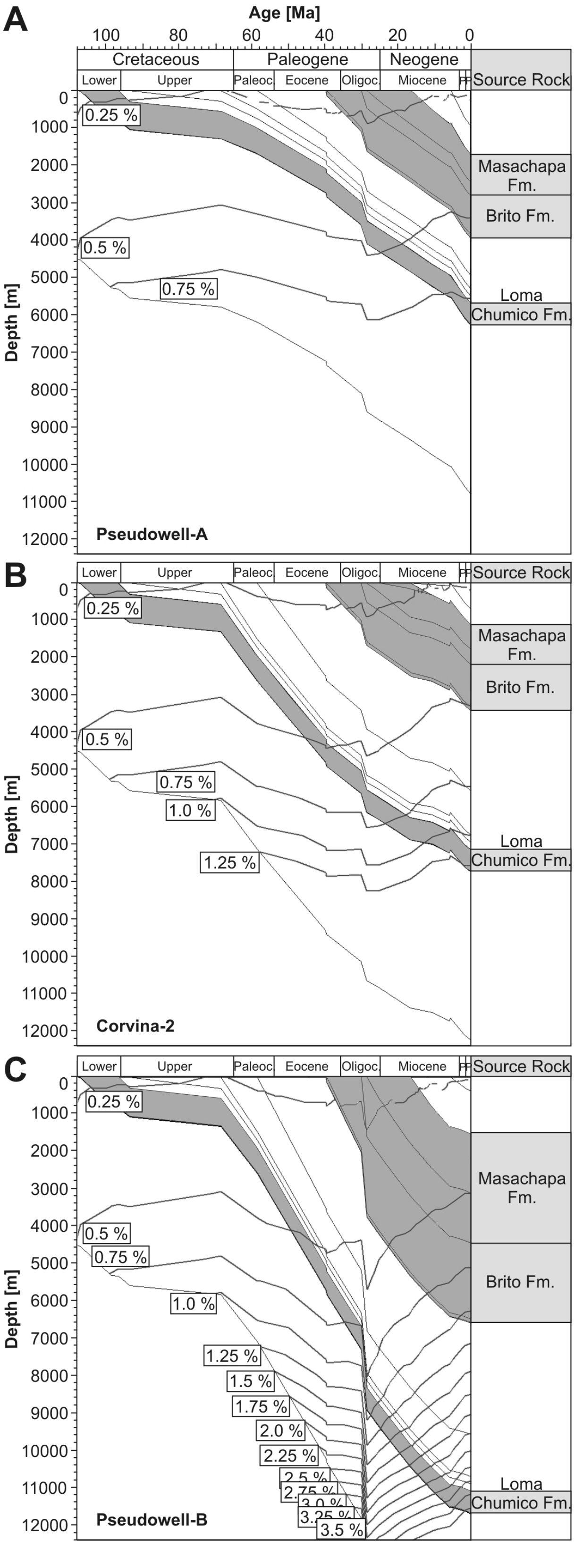

Fig. 10. Burial history along the modelled cross-section at: A. pseudo-well A (Grid Point 215); B. well *Corvina-2* (Grid Point 263); and C. pseudo-well B (Grid Point 392). The overlay shows isolines of organic matter maturation calculated as vitrinite reflectance (EASY%Ro, Sweeney and Burnham, 1990). For location of the 1D models, see Fig. 2B.

depocentre was modified during the Oligocene as the Corvina and Argonaut anticlines developed due to transpressional folding and uplift (Ranero *et al.*, 2000b), dividing the basin into inner, deeper and western, shallower parts (Fig. 9C). In the Late Oligocene, during deposition of the Masachapa Formation, maximum sedimentation rates were reached in the inner basin (1,563 m/Ma). Since the Late Miocene, the area of the present-day coast has been affected by tectonic uplift. In contrast, the basin continued to subside and began to shift seawards as a result of coastal uplift (Fig. 9D-E). According to Ranero *et al.* (2000b), subsidence was caused by "subduction erosion" of the upper plate.

As a result of burial history modelling, three phases of enhanced subsidence are recognised (Late Eocene, Late Oligocene and Plio-Pleistocene), with the highest subsidence occurring during the Late Oligocene (Fig. 10).

Thermal modelling results suggest that the deep parts of the basin are relatively cool due to the generally low basal heat flow and the low geothermal gradient. A constant basal heat flow of 39 mW/m^2 was reconstructed resulting in a good fit between measured and calculated vitrinite reflectance. This corresponds well to the typical heat flow of forearc basins which ranges from 20 to 45 mW/m^2 and a mean of 35 mW/m^2 (Allen and Allen, 2005).

Within the deep part of the basin, temperatures of the Lower Cretaceous Loma Chumico Formation range from 249°C at the base to 235°C at the top of the formation (Fig. 11). The Middle Eocene to Lower Oligocene Brito Formation has a temperature range of 149°C at the base to 109°C at the top. The temperature of the top of the directly overlying Upper Oligocene to Lower Miocene Masachapa Formation is only 57°C. With the exception of the uplifted NE sector, the sedimentary succession in the Sandino Basin has reached its maximum temperatures and maturities at the present day, with the highest values in the deepest parts of the basin. Here, maturities of up to 3.6 % Rr were calculated for the base of the Lower Cretaceous Loma Chumico Formation (Fig. 10). From thermal calibration, Fig. 11 illustrates the modelled temperature distribution along the seismic section, with present-day temperature gradients ranging between 24 and 28°C/km. This is in good agreement with results from INE internal studies which show geothermal gradients between 24 and 30°C/km, with an average of 29°C/km for the offshore part of the basin.

Petroleum generation

Geochemical evaluation of cuttings samples from well *Corvina-2* indicated that the Brito and Masachapa Formations have source rock potential. These source

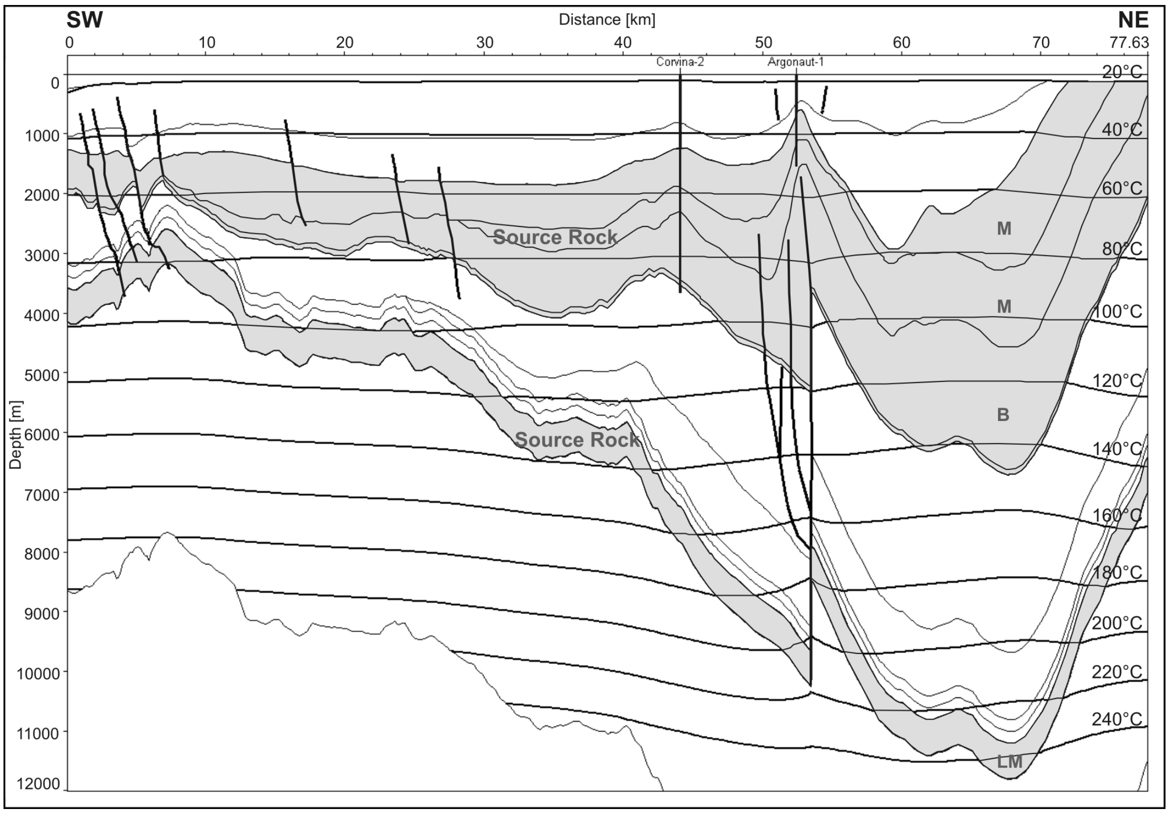

Fig. 11. Recent temperature distribution along the modelled section (LC: Loma Chumico Formation; B: Brito Formation; M: Masachapa Formation). The thin solid lines delineate stratigraphic boundaries.

rocks reach maximum burial depths and highest maturities in the centre of the basin near the present-day coastline (Fig. 10C). At the *Corvina-2* location, the onset of petroleum generation (>0.5 %Rr) is estimated to occur at a depth of approximately 3,200 m below seafloor, within Upper Eocene sediments of the Brito Formation. Within the deep part of the basin, the top of the oil window is reached in Upper Oligocene sediments of the Masachapa Formation. The maturity of the underlying Brito Formation is significantly higher and corresponds to a later stage of oil generation (>1 % Rr).

The conversion of kerogen to petroleum was modelled using specific reaction kinetics for potential source rocks in the Brito and Masachapa Formations. Hydrocarbon generation from the Loma Chumico Formation remains speculative, because the existence of this unit along the investigated cross-section has not yet been established. For the purposes of modelling, this interval was assigned with previously-published geochemical characteristics (Astorga, 1997; Darce *et al*., 2000b; Table 3), and a standard kinetic model (Burnham and Sweeney, 1989) was applied. Different scenarios were tested by integrating measured data with data from more speculative source rock intervals. Results indicate that both the Brito and Masachapa Formations contain productive source rock intervals within the deep part of the basin. In contrast, at well *Corvina-2*, the Masachapa Formation has not reached sufficient burial depths to generate hydrocarbons (Fig. 12). Therefore, the deep basin can be regarded as a potential kitchen area.

The timing of petroleum generation for the proven and hypothesized source rocks is illustrated in Figs 12 and 13. Considering the reconstructed structural and thermal history of the cross-section, the timing of petroleum generation for the different source rocks within the deepest portion of the basin was investigated. The Lower Cretaceous black shales of the Loma Chumico Formation have already realised most of their petroleum potential over large parts of the section, and for this formation the main phase of petroleum generation lasted from the Late Eocene to the end of the Early Oligocene (39.5-30 Ma). The highest rates of petroleum generation were reached at the beginning of the Oligocene, and the primary generation of oil has ceased at the present day. Secondary cracking to gas may occur in the deep basin. The Middle Eocene to Lower Oligocene Brito Formation source rocks reached their main phase of petroleum generation at the beginning of the Late Oligocene (30 Ma), with highest rates occurring in the Middle Miocene (16.5 Ma). Some 50 to 90 % of the overall hydrocarbon generation potential of the Brito Formation has been realized at the present day leaving only a residual capacity. The Upper Oligocene to Lower Miocene Masachapa Formation entered the main phase of petroleum generation during the Early

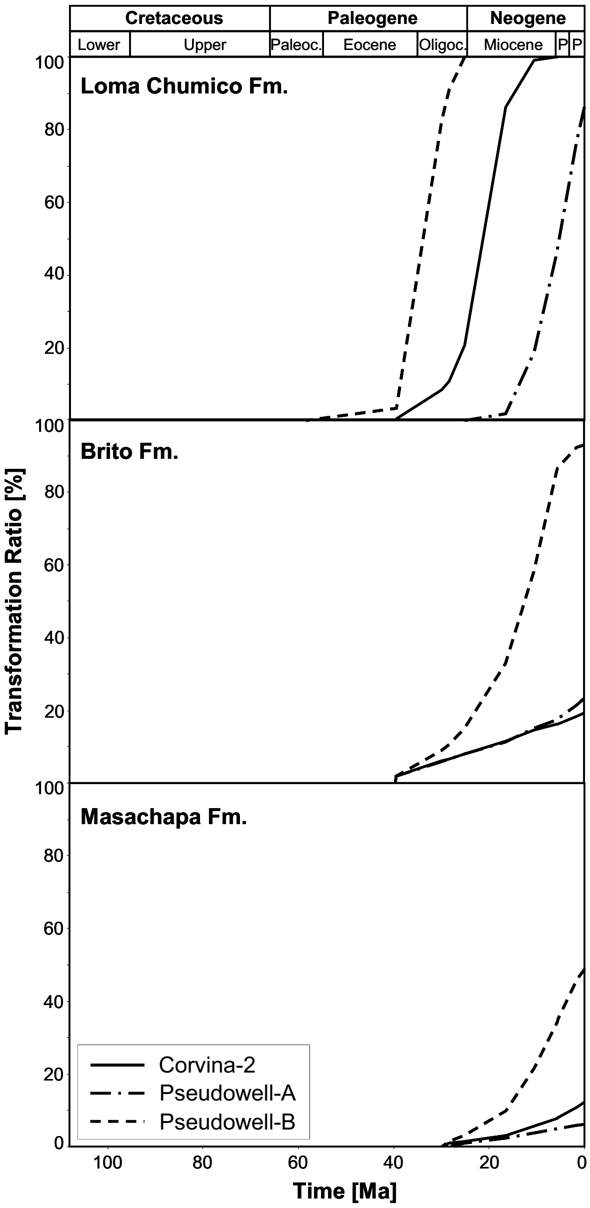

Fig. 12. Timing of petroleum generation of the three potential source rocks at different Grid Points along the seismic section: at the centre of the section at pseudowell-A (Grid Point 215); at well *Corvina-2* (Grid Point 263); and in the deep part of the basin at pseudowell-B (Grid Point 392). For the exact locations of the wells, see Fig. 2B.

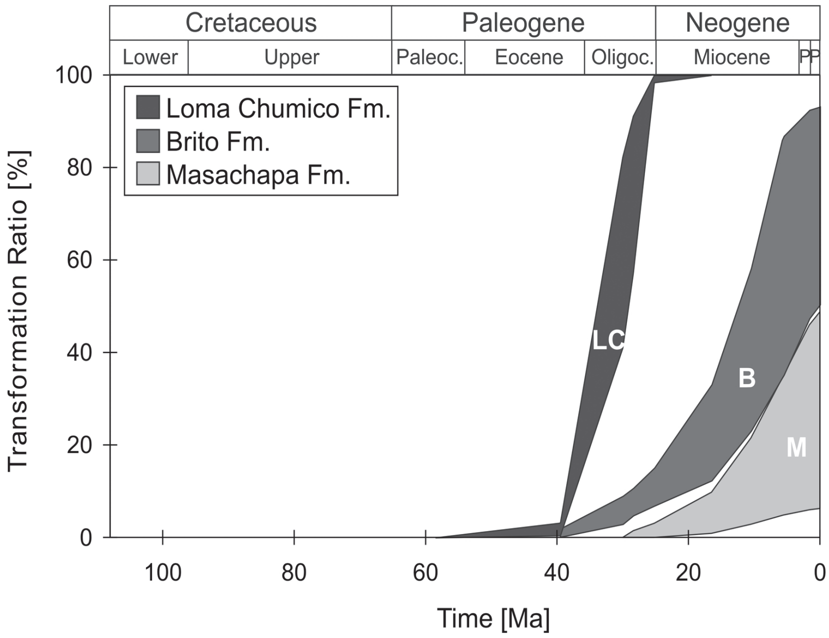

Fig. 13. Timing of petroleum generation of the three potential source rocks expressed as transformation ratio in percent of total potential within the deep part of the basin at pseudowell-B (GP 392) (location: Fig. 2B). The shaded fields illustrate the range of the transformation ratio from the base to the top of each formation.

Fig. 14. Petroleum migration pathways modelled with optimum values at different times of basin evolution (green arows: liquid flow paths; red arrows: vapour flow paths). A. Late Oligocene; B. Early Miocene; C. Late Miocene; and D. Recent.

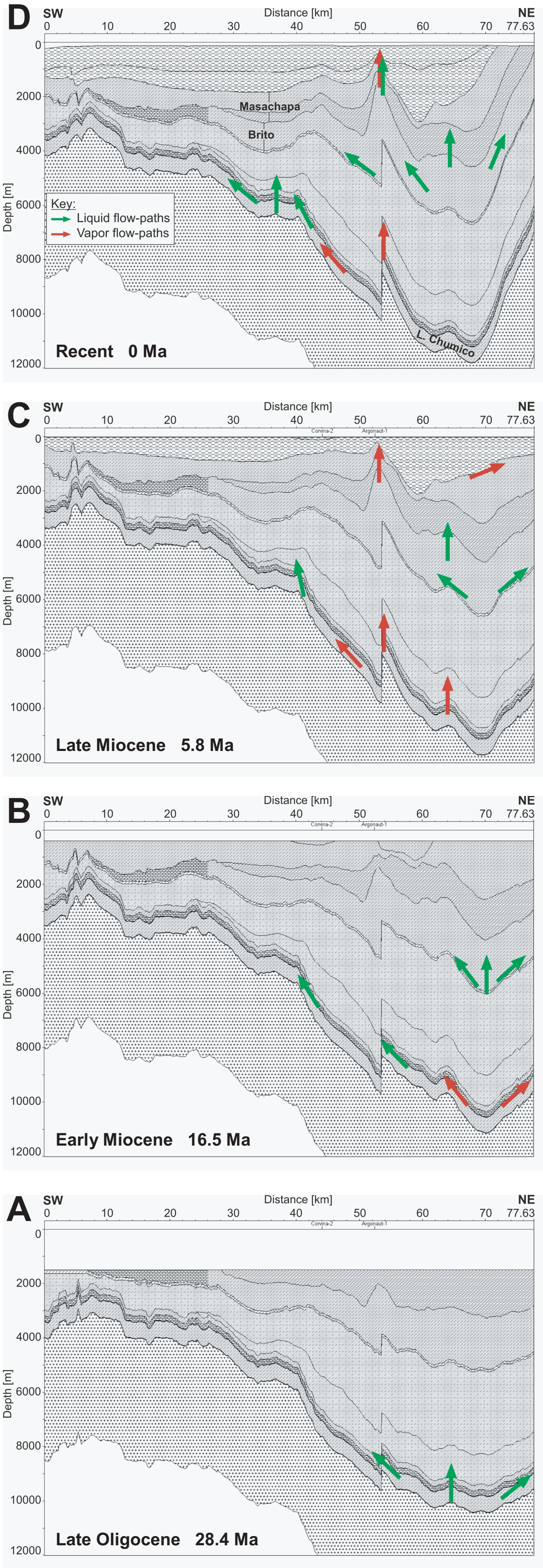

Miocene (ca. 20 Ma), and is continuing to generate hydrocarbons. Depending on the precise location along the profile, up to 50 % of the potential of the Masachapa Formation has been realized (Fig. 12).

Petroleum migration and trapping

Modelling indicates that the main phase of petroleum generation for the known and hypothesized source rocks coincides with phases of maximum subsidence associated with the highest sedimentation rates. The expulsion of hydrocarbons from the various source rocks will be concentrated in the kitchen area in the deep basin. The first hydrocarbons may have been expelled at the end of the Eocene (around 36 Ma) from the hypothesized Loma Chumico Formation source rock. According to the model, the Brito Formation began to expel hydrocarbons during the Early Miocene (around 20 Ma), while expulsion from the Masachapa Formation source rocks started in the Late Miocene (around 8 Ma), although no hydrocarbon expulsion from the uppermost part of the formation is taking place at the present day. Hydrocarbons that were expelled prior to the formation of the coastal flexure in the Late Miocene probably escaped directly to the surface.

Fig. 14 shows the main 2D migration pathways of oil and gas along the modelled cross-section. Petroleum migration was modelled in *PetroMod* applying Darcy flow. Until the Late Oligocene (Fig. 14A), migration of petroleum from the hypothesized Loma Chumico Formation source would have taken place from the kitchen in a vertical direction or laterally towards the flanks of the subsiding basin. Until the Middle Miocene, the migration path from the kitchen area towards the SW and NE margins of the cross-section did not change significantly. Oil from the Brito Formation is also modelled to follow upward and lateral migration paths within the deep basin (Fig. 14B). Oil and gas from the Loma Chumico Formation is modelled to continue to migrate updip to the SW as well as along faults in the area of the Argonaut anticline (Fig. 14C and D). Oil from the Brito Formation migrated towards the basin centre, and also vertically along faults around the Argonaut anticline (Fig. 14D). This is consistent with the oil and gas shows reported from the *Corvina-2* and *Argonaut-1* boreholes.

We therefore assume that the deep basin and the NE flank of the Argonaut anticline are likely to represent the main petroleum migration pathways along the modelled section. In this area, traps may have formed due to fault activity and high sediment accumulation rates which coincided with the expulsion of hydrocarbons from the Loma Chumico Formation in the Late Eocene. The occurrence of reservoir rocks with suitable porosity and permeability characteristics, however, remains speculative.

Faults can act as potential seals or migration pathways for fluid flow, depending on phases of increased fault activity (e.g. Poelchau *et al*., 1997). There is as yet insufficient information about the modelled seismic section to be able to decide whether the fault zones around the Argonaut anticline permitted pressure communication and fluid flow. Porosity and permeability measurements are not available, but drilling reports from wells *Argonaut-1* and *Corvina-2* indicate an overpressured environment. In the area around the Argonaut anticline, abnormally high pressures may be related to shale diapirism (INE, *internal reports*). Shale smearing along faults may have inhibited fluid flow across the fault zone.

To evaluate the effects on petroleum migration, we tested a number of transmissibility scenarios within the Argonaut area for times of increased fault activity. The modelled structural development of the seismic section indicates highest rates of fault juxtaposition within the Argonaut area during the Late Eocene to Late Oligocene (39.5 to 28.4 Ma) and the Early Miocene (25.2 to 16.5 Ma). During these times, the vertical and lateral transmissibilities of the 2D model were set in different model runs either to "completely open" or to "completely closed". However, the different fault properties gave no indication of enhanced or reduced fluid flow across the Argonaut anticline. Basin modelling demonstrates that this area most probably played a minor role in petroleum migration, and suggests that migration pathways remained focussed along the inner flanks of the deep basin.

DISCUSSION

The hydrocarbon potential of forearc basins is conventionally considered to be low. This is in general based on the limited occurrence or absence of coal or other organic-rich intervals, low geothermal gradients, and the paucity of porosity due to diagenetic factors (e.g. Dickinson, 1995). The Sandino Basin is, however, thermally mature, and generation potential is associated with organic-rich intervals in the Brito and Masachapa Formations. The existence of Lower Cretaceous source rocks (Loma Chumico Formation) has not been shown in the Sandino Basin and must therefore be treated as hypothetical. Petrographic analyses by INE (*unpublished*) document a higher proportion of mature sandstones in the upper parts of the basin fill, and the presence of calcite cementation and secondary porosity favour the occurrence of reservoir potential. Recent petrographic analyses of core samples from deep-water sandstones of the Brito Formation (Norwood Resources Ltd) have indicated porosities of 16-24 % and permeabilites of up to 75

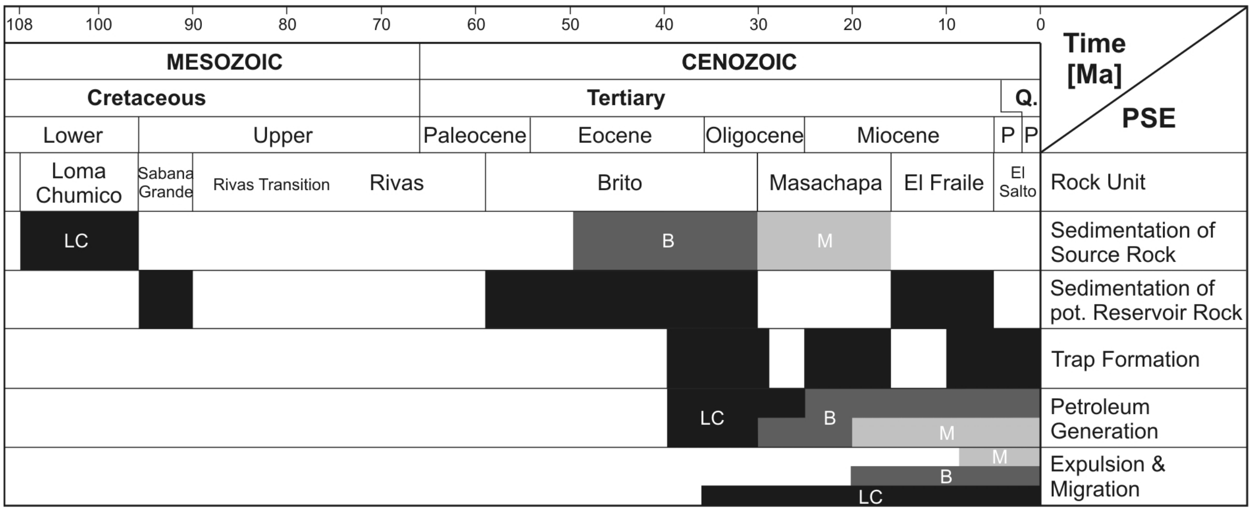

Fig. 15. Petroleum system events chart for the Sandino Basin (LC: Loma Chumico Formation; B: Brito Formation; M: Masachapa Formation).

mD. Fig. 15 summarises the main petroleum system elements of the Sandino Basin, illustrating the results of petroleum generation modelling.

Basin modelling reveals that, with the exception of the uplifted NE sector, the sedimentary succession in the Sandino Basin has reached its maximum temperatures and maturities at the present day, with the highest values in the deepest parts of the basin. Here, modelling of the hydrocarbon generation from the different source rock intervals demonstrates that the Loma Chumico Formation has already reached a post-mature stage with a calculated maturity of 3.6 % Rr at its base (cf. Peters and Cassa, 1994; Fig. 10C). Today, the primary generation of oil has ceased but secondary cracking to gas is assumed to occur within the deep part of the basin due to high temperatures ranging from 249°C at the base and 13°C at the top of the Loma Chumico Formation (Fig. 11). It can further be shown that the Brito and Masachapa Formations have reached the top of the oil window within a depth of approximately 2000 m along the investigated seismic line. The top of the gas window is reached in the deepest part of the basin within the upper part of the Brito Formation at a depth of approximately 5000 m (Fig. 11), with the Brito Formation already being in a peak to late stage of thermal maturity (0.75 % Rr, Fig. 10C).

The quality of a basin modelling study's results strongly depends on the quality and quantity of the input parameters. For the basin modelling study presented here, most important geological information was extracted from the seismic section and the well reports of well *Corvina-2*. This well limits our knowledge of the offshore stratigraphy and lithology of the Sandino Basin to a total depth of 3,666 m within sediments of Middle Eocene age. About half of the sedimentary sequence remains undrilled and for these deeper sequences the model has to rely mainly on seismic interpretation and extrapolations from onshore outcrops. From these extrapolations, we infer that the deeper undrilled stratigraphic intervals may also act as source rocks. Due to the limited database, the spatial extent and thickness of the defined source rocks remain speculative along the entire section. However, according to wells *Rivas-1* and *El Ostional-1,* which encountered sediments of the Loma Chumico Formation, Cretaceous black shales are expected to be present over a considerable part of the Sandino Basin.

Quantitative predictions on the petroleum migration and saturation of filled reservoirs were not possible because of the limited data-base and the lack of porosity and permeability measurements. In addition, quantification of petroleum volumes always remains speculative along 2D image planes. Therefore, quantitative aspects of the petroleum system analysis were excluded from this study.

CONCLUSIONS

Geochemical analyses of cuttings samples from the Sandino Forearc Basin indicate the presence of potential source rock intervals in Middle Eocene to Lower Oligocene sediments of the Brito Formation and Upper Oligocene to Lower Miocene sediments of the Masachapa Formation. TOC values range between 1.9 and 3.2 %. The sedimentary organic matter is a mixed Type II-III kerogen with increasing contributions of sapropelic kerogen within the Brito Formation.

Maturity data from a borehole in the mid-basin anticlinal area indicate that the Brito Formation has reached a stage of thermal maturity below a depth of 3400 m. In contrast, the Masachapa Formation is still thermally immature.

Thermal history modelling points to a constant basal heat flow of 39 mW/m2 and a temperature gradient ranging between 24°C and 28°C/km. The oldest assumed source rock interval, the Loma Chumico Formation, reaches temperatures of 235-249°C at the present day (maturity of 3.6 % Rr).

The conversion of kerogen to petroleum was modelled using sample-specific reaction kinetics for potential source rocks in the Brito and Masachapa Formations. Basin modelling shows that these source rocks, including hypothesized Loma Chumico source rocks, reach highest petroleum productivities within the deep part of the basin. Therefore, a petroleum kitchen is proposed in the deepest part of the Sandino Basin.

Peak generation by source rocks in the Lower Cretaceous Loma Chumico Formation was modelled to have occurred since the Late Eocene. The main phase of petroleum generation from the Brito source rocks occurred at the beginning of the Late Oligocene with an onset of expulsion in the Early Miocene. The Masachapa source rocks entered the main phase of petroleum generation during the Early Miocene and, in large portions of the section, are still continuing to generate hydrocarbons.

Phases of maximum petroleum generation for the calculated drilled and hypothesized source rocks largely coincide with phases of maximum subsidence in the Late Eocene, Late Oligocene and Plio-Pleistocene, and with associated high sedimentation rates.

Pathways for hydrocarbon migration are predicted to be concentrated between the deepest part of the basin and the flanks. According to the modelling results, substantial volumes of petroleum may have been lost from the investigated section through the uplifted NE margin and through the surface.

ACKNOWLEDGEMENTS

This study was supported by grants from the German Academic Exchange Service (DAAD) and the Leibniz University Hannover ("Freundeskreis der Leibniz Universität Hannover e.V." and "GradFÖG"). It was undertaken in the framework of collaboration between the Leibniz University Hannover, the Federal Institute for Geosciences and Natural Resources BGR ("Bundesanstalt für Geowissenschaften und Rohstoffe"), Hannover, and the Nicaraguan National Insitute for Energy INE ("Instituto Nicaragüense de Energía"), Managua. The authors are grateful to Cesar Ranero and the Leibniz Institute of Marine Sciences (IFM-GEOMAR) for permission to publish the reprocessed seismic line ST8910-215. They thank colleagues from INE for their assistance in data acquisition and logistic support. Georg Scheeder and Werner Hiltmann (BGR) are thanked for support during lab work and petrographical analysis, respectively. Ingolf Dumke is acknowledged for his assistance with the Pyrocalc software. Discussions with Stefan Grassmann, Claudius Vandré and Christian Brandes are acknowledged.

The manuscript benefited considerably from comments and suggestions by Christoph Heubeck and an anonymous referee, which are gratefully acknowledged.

REFERENCES

ALLEN, P.A. and ALLEN, J.R., 2005. Basin Analysis: Principles and applications. Blackwell, Oxford, 549 pp.

ASTORGA, A., 1987. El Cretácico Superior y el Paleógeno de la vertiente Pacifica de Nicaragua meridional y Costa Rica septentrional: Origen, evolución y dinámica de las cuencas profundas relacionadas al margen convergente de Centroamérica. MSc Thesis, Univ. Costa Rica, San José, Costa Rica, 115.

ASTORGA, A., 1988. Geodinámica de las cuencas del Cretácico Superior-Paleógeno de la región "forearc" del sur de Nicaragua y Norte de Costa Rica. *Rev. Geol. Amer. Central*, **9**, 1-40.

ASTORGA, A., 1990. La Formacion Loma Chumico (Complejo de Nicoya, Costa Rica) y su relación con la evolución cretácica del margen oeste del "paleo-plateau" Caribe (abstract). VII Congreso Geológico de América Central, Resumen, 128 pp.

ASTORGA, A., 1994. El Mesozoico del sur de América Central: consecuencias para el origen y evolución de la Placa Caribe. In: SEYFRIED, H. and HELLMANN, W. (Eds.): Geology of an Evolving Island Arc: The Isthmus of Southern Nicaragua, Costa Rica and Western Panamá. Profil, Univ. Stuttgart, **7,** 171-233.

ASTORGA, A., 1997. El puente-istmo de América Central y la evolución de la Placa caribe (con éfasis en el Mesozoico). Ph.D. thesis, Univ. Stuttgart, *Profil*, **12,** 1-201.

ASTORGA, A., FERNANDEZ, J.A., BARBOZA, G., CAMPOS, L., OBANDO, J., AGUILAR, A. and OBANDO, L.G., 1991. Cuencas sedimentarias de Costa Rica: Evolución géodinamica y potential de hidrocarburos. *Rev. Geol. Amer. Central*, **13,** 15-59.

BAUMGARTNER, P.O., MORA, C.R., BUTTERLIN, J., SIGAL, J., GLACON, G., AZÉMA, J. and BOURGOIS, J. 1984. Sedimentación y paleografia del Cretácico y Cenozoico del litoral pacífico de Costa Rica. *Rev. Geol. Am. Central* **1**, 57-136.

BOURGOIS, J., AZEMA, J., BAUMGARTNER, J., DESMET, P:O. and AUBOIN, J. 1984. The geologic history of the Caribbean-Cocos plate boundary with special reference to the Nicoya Complex (Costa Rica) and DSDP results (Legs 67 and 84 off Guatemala): a synthesis. *Tectonophysics*, **108,** 1-32.

BURNHAM, A.K. and SWEENEY, J.J., 1989. A chemical kinetic model of vitrinite maturation and reflectance. *Geochim. Cosmochim. Acta*, **53**, 2649-2657.

CALVO, C., 2003. Provenance of plutonic detritus in cover sandstones of Nicoya Complex, Costa Rica: Cretaceous unroofing history of a Mesozoic ophiolite sequence. *GSA Bull.*, **115**, 832-844.

CROWE, J.C. and BUFFLER, R.T., 1985. Multichannel seismic records across the Middle America Trench and Costa Rica-Nicaragua convergent margin. NCY-7 NCI-1. In: LADD, J.W. and BUFFLER, R.T. (Eds.): Middle America Trench off Western Central America Ocean Drilling Program. Reg.

Dat Syn. Ser., Atlas 7, Mar. Sct. Int., 11 pp.

DARCE, M., BACA, D., DUARTE, M., BARBOZA, G. and FERNÁNDES, A., 2000 a. New concepts point toward oil, gas potential in Nicaragua. *Oil & Gas J.*, **98**, 69-73.

DARCE, M., BACA, D. and DUARTE, M., 2000 b. New law, seismic information smooth Nicaragua licensing. *Oil & Gas J.,* **98,** 72-74.

DENGO, G., 1962. Estudio Geológico de la Región de Guanacaste, Costa Rica. Instituto Geográfico Nacional, San José, Costa Rica, 112.

DICKINSON, W.R., 1995. Forearc basins. In: BUSBY, C.J. and INGERSOLL, R.V., (Eds.), Tectonics of Sedimentary Basins. Blackwell, Oxford, 221-262.

ERLICH, R.N., ASTORGA, A., SOFER, Z., PRATTS, L.M. and PALMER, S.E., 1996. Palaeoceanography of organic-rich rocks of the Loma Chumico Formation of Costa Rica, Late Cretaceous, eastern Pacific. *Sedimentology*, **43**, 691-718.

ESPITALIE, J., 1986. Use of Tmax as a maturation index for different types of organic matter. Comparison with vitrinite reflectance. In: BURRUS, J. (Ed.): Thermal Modeling in Sedimentary Basins. Editions Technip, Paris, 475-496.

ESPITALIE, J., LAPORTE, J.L., MADEC, M., MARQUIS, F., LEPLAT, P. and PAULET J., 1977. Méthode rapide de caractérisation de roches mères, de leur potentiel pétrolier et de leur degré d'évolution. *Rev. IFP*, **32**, 23-45.

ESPITALIE, J., DEROO, G., and MARQUIS, F., 1986. La pyrolyse rock-eval et ses applications (troisiéme partie). *Revue de l'Institute Francais du Pétrole,* **41**, 73-89.

FRISCH, W., MESCHEDE, M.and SICK, M. 1992. Origin of the Central American ophiolites: evidence from paleomagnetic results. *Bull. Geol. Soc. Am.*, **104,** 1301-1314.

GALLI-OLIVIER, C. and SCHMIDT-EFFING, R., 1977. Estratigrafía de la cubierta sedimentaria supra-ofiolítica Cretácica de Costa Rica. *Ciencia y Technología (J. of the Univ. Costa Rica)*, **1,** 87-96.

GALLI-OLIVIER, C. 1979. Ophiolite and island-arc volcanism in Costa Rica. *Bull. Geol. Soc. Am.*, **90,** 444-452.

GURSKY, H.-J. and SCHMIDT-EFFING, R., 1983.Sedimentology of radiolarites within the Nicoya Complex, Costa Rica, Central America. In: IIJIMA, A., HEIN, J.R. and SIEVER, R. (Eds.): Siliceous Deposits in the Pacific Region. *Developments in Sedimentology*, **36,** Elsevier, Amsterdam, 127-142.

HANDSCHUMACHER, D.W., 1976. Post-Eocene plate tectonics of the eastern Pacific. In: SUTTON, G.H., MANGHNANI, M.H. and MOBERLY, R. (Eds.): The Geophysics of the Pacific Ocean Basin and its Margin: a volume in Honor of P.Woollard. Monogr. *Am. Geophys. Union*, **19**, AGU, Washington DC., 177-202.

HAQ, B.U. and VAN EYSINGA, F.W.B., 1987. Geologic Time Table. 4th edn. Elsevier, Amsterdam.

HAYES, C.W., 1899. Physiography and geology of the region adjacent to the Nicaragua canal route. *Bull. Geol. Soc. Am.,* **10**, 285-348.

HOFFSTETTER, R., DENGO, G. and WEYL, R., 1960. Costa Rica. In: HOFFSTETTER, R. (Ed.): Lexique Stratigraphique International, Amérique Central. Centre National de la Recherche Scientifique (CNRS), París, Fascícul. 2.5, 223-306.

HUENE, R. VON and FLUEH, E., 1994. A review of marine geophysical studies along the Middle America Trench off Costa Rica and the problematic seaward terminus of continetal crust. In: SEYFRIED, H. and HELLMANN, W. (Eds.): Geology of an Evolving Island Arc, The Isthmus of Southern Nicaragua, Costa Rica and Western Panamá. *Profil,* **7**, 143-159.

IHS, 2007. Nicaragua. *International Oil Letter*, **23**, 7th May 2007.

JOY, O.T., 1941. Structure and Stratigraphy of the Rivas area. Managua, 25-47.

KOLB, W., 1990. Die Neogene Schelf-Sedimentation in Südwest-Nicaragua: Ablagerungssequenzen und paläographische Szenarien. Institut für Geologie und Paläontologie der Universität Stuttgart, 161 pp.

KOLB, W. and SCHMIDT, H., 1991. Depositional sequences associated with equilibrium coastlines in the Neogene of southwest Nicaragua. In: MACDONALD, D.I.M. (Ed.): Sea-Level Changes at Active Plate Margins: Processes and Products. *Spec. Publ. IAS,* **12**, 259-272.

KRAWINKEL, H. and KOLB, W., 1994. Sequential aspects of the Neogene El Fraile formation (Nicaragua Trough, SW-Nicaragua). In: SEYFRIED, H. and HELLMANN, W. (Eds.): Geology of an evolving island arc. *Profil,* **7**, 325-333.

KRAWINKEL, H., SEYFRIED, H., CALVO, C. and ASTORGA, A., 2000. Origin and inversion of sedimentary basins in southern Central America. *Zeitschrift für Angewandte Geologie, Sonderheft SH* **1,** 71-77.

KUANG, S.J., 1971. Estudio geológico del Pacífico de Nicaragua. Catastro de Inventario de Recursos Naturales, División de Geología, Managua, *Informe Geológico*, **3**, 1-101.

KUMPULAINEN, R.A., 1995. Stratigraphy and Sedimentology in Western Nicaragua. *Rev. Geol. Amer. Central*, **18**, 91-94.

KUMPULAINEN, R.A., HÖGDAHL, K., ÓLAFSSON, G., MUOZ, A. and VALLE, M., 1999. Sedimentology and stratigraphy of the fore-arc basin in SW Nicaragua. In: ELMING, S.Å., WIDENFALK, L. and RODRIGUES, D. (Eds.): Geoscientific Research in Nicaragua: Swedish-Nicaraguan joint project during the period 1981-1991. Luleå Technical University, Sweden, 107-116.

LANGFORD, F.F. and BLANC-VALLERON, M.-M., 1990. Interpreting Rock-Eval pyrolysis data using graphs of pyrolizable hydrocarbons vs. total organic carbon. *AAPG Bull.*, **74,** 709-804.

LUNDBERG, N., 1982. Evolution of the slope landward of the Middle America Trench, Nicoya Peninsula, Costa Rica. In: LEGETT, J.K. (Ed.): Trench-forearc geology. *Spec. Publ. Geol. Soc. London*, **10,** 131-147.

LUNDBERG, N., 1991. Detrital record of the early Central American magmatic arc: Petrography of intraoceanic forearc sandstones, Nicoya Peninsula, Costa Rica. *Bull. Geol. Soc. Am.*, **103**, 905-915.

MACDONALD, D.F., 1920. Informe final geológico de Costa Rica. *Rev. de Costa Rica,* **2**, 28-32, 50-57, 106-111, 123-125, 139-148 [Reproduced from the Gaceta Oficial, June 1919]].

MANN, P. and KOLARSKI, R.A., 1995. East Panama deformed belt: Structure, age, and neotectonic significance. In: MANN, P. (Ed.): Geologic and Tectonic Development of the Caribbean Plate Boundary in Southern Central America. *Spec. Pap. Geol. Soc. Am.*, **295**, 111-130.

MCINTOSH, K., AHMED, I., SILVER, E., KELLY, R., RANERO, C.R., FLUEH, E. and BERHORST, A., 2002. Nicaragua/Costa Rica Marine Geophysics Update. Margins Newsletter, 8, Spring 2002, 3-5.

PETERS, K.E., 1986. Guidelines for evaluating petroleum source rock using programmed pyrolysis. *AAPG Bull.*, **70**, 318-329.

PETERS, K.E. and CASSA, M.R., 1994. Applied source rock geochemistry. In: MAGOON, L.B. and DOW, W.G. (Eds.): The Petroleum System: From Source to Trap. *AAPG Memoir*, **60**, 93-120.

PINDELL, J.L. and BARETT, S.F., 1990. Geological evolution of the Caribbean region; A plate-tectonic perspective. In: DENGO, G. and CASE, J.E. (Eds.): The Geology of North America (Vol. H), The Caribbean Region. Geol. Soc. Am., Boulder, Colorado, 405-432.

POELCHAU, H.S., BAKER, D.R., HANTSCHEL, T., HORSFIELD, B. and WYGRALA, B.P., 1997. Basin simulation and the design of the conceptual basin model. In: WELTE, D.H., HORSFIELD, B. and BAKER, D.R. (Eds.): Petroleum and Basin Evolution. Springer, Berlin, 2-62.

PROTTI, M., GUENDEL, F. and MCNALLY, K., 1995. Correlation between the age of the subducting Cocos plate and the geometry of theWadati-Benioff zone under Nicaragua and

Costa Rica. In: MANN, P. (Ed.): Geologic and Tectonic Development of the Caribbean Plate Boundary in Southern Central America. *Geol. Soc. Am. (Spec. Pap.),* **295**, 309–326.

RADKE, M., HORSFIELD, B., LITTKE, R. and RULLKÖTTER, J., 1997. Maturation and petroleum generation. In: WELTE, H., HORSFIELD, B. and BAKER, D.R. (Eds.): Petroleum and Basin Evolution. Springer, Berlin, 169-229.

RANERO, C.R., HUENE, R. VON, FLUEH, E.R., WEINREBE, W., HINZ, K., LEANDRO, G., ALVARADO, G. and DUARTE, M., 2000 a. Lower Plate Control on Subduction Erosion Processes along the Middle America Convergent Margin. *Zeitschrift für Angewandte Geologie*, SH **1**, 71-77.

RANERO, C.R., HUENE, R. VON, FLUEH, E., DUARTE, M., BACA, D. and MCINTOSH, K., 2000 b. A cross section of the convergent Pacific margin of Nicaragua. *Tectonics,* **19**, 335-357.

SCHMIDT-EFFING, R., 1979. Alter und Genese des Nicoya-Komplexes, einer ozeanische Paläokruste (Oberjura bis Eozän) im südlichen Zentralamerika. *Geol. Rdsch*., **68**, 457-494.

SEYFRIED, H., ASTORGA, A., AMANN, H., CALVO, C., KOLB, W., SCHMIDT, H. and WINSEMANN, J., 1991. Anatomy of an evolving island arc: tectonic and eustatic control in the south Central American forearc area. In: MACDONALD, D.I.M. (Ed.): Sea-Level Changes at Active Plate Margins: Processes and Products. *Spec. Publ. IAS*, **12**, 273-292.

STRUSS, I., BRANDES, C., BLISNIUK, P. and WINSEMANN, J., 2007. Eocene deep-water channel-levee deposits, Nicaragua: channel geometries and internal deformation patterns of six outcrops. In: NILSEN, T.H., SHEW, R.D., STEFFENS, G.S. and STUDLICK, J.R.J. (Eds.): Atlas of Deep-water Outcrops. *AAPG Studies in Geology*, **56,** CD Rom, 31 pp.

STRUSS, I., CRAMER, B., DUARTE MORALES, M., VANDRÉ, C. and WINSEMANN, J., *in press*. Depositional environment and source rock potential of the Masachapa Formation, Sandino forearc Basin, Nicaragua. *Journ. South Am. Earth Sc.*

SWEENEY, J.J. and BURNHAM, A.K., 1990. Evaluation of a simple model of vitrinite reflectance based on chemical kinetics. *AAPG Bull.,* **74**, 1559- 1570.

TAYLOR, G.H., TEICHMÜLLER, M., DAVIS, A., DIESSEL, C.F. K., LITTKE, R. and ROBERT, P.**,** 1998. Organic Petrology. Gebr. Borntraeger, Berlin-Stuttgart, 704 pp.

TISSOT, B.P. and WELTE, D.H., 1984. Petroleum Formation and Occurrence. Spinger-Verlag, 699 pp.

WALTHER, C.H.E., FLUEH, E.R., RANERO, C.R., VON HUENE, R. and STRAUCH, W., 2000. Crustal structure across the Pacific margin of Nicaragua: evidence for ophiolitic basement and a shallow mantle sliver. *Geophys. J. Intern*., **141,** 759-777.

WEINBERG, R.F., 1992. Neotectonic development of western Nicaragua. *Tectonics,* **11**, 1010-1017.

WEYL, R., 1980. Geology of Central America. Borntraeger, 371 pp.

WILSON, T.C., 1941. Reconnaissance geology of southwestern portion of department of Carazo. Unpublished report, Managua, 7-13.

WILSON, T.C., 1942. Summary Report on the geology of the Pacific coast area – Nicaragua: Part I, General Geology. *Unpublished report*, Managua, 1-27.

WILSON, T.C. and FAGGINGER-AUER, W., 1942. Summary report on the geology of the Pacific coast area – Nicaragua: Part II, Laboratory Analysis. *Unpublished report*, 28-43.

WINSEMANN, J. and SEYFRIED, H., 1991. Response of deep-water forearc systems to sea-level changes, tectonic activity and volcaniclastic input in Central America. In: MacDONALD, D.I.M. (Ed.): Sea-Level Changes at Active Plate Margins: Processes and Products. *Spec. Pub. IAS,* **12**, 217-240.

WINSEMANN, J., 1992. Tiefwasser-Sedimentationsprozesse und -produkte in den Forearc-Becken des mittelamerikanischen Inselbogensystems: eine sequenzstratigraphische Analyse. Ph.D. thesis, Univ. Stuttgart, *Profil,* **2**, 218 pp.

WYGRALA, B.P., 1989. Integrated study of an oil field in the southern Po basin, northern Italy. Ph.D. thesis, Univ. Köln, Berichte Kernforschungsanlage Jülich, 2313, 1-217.

ZOPPIS BRACCI, L. and DEL GIUDICE, D., 1958. Geolgogía de la costa del Pacífico de Nicaragua. *Boletín del Servicio Geológico Nacional, Nicaragua*, 17-48.